

CLIMATOLOGICAL TRAJECTORY ANALYSIS OF AIR POLLUTION FROM  
ISTANBUL TO ITS SURROUNDINGS

BAHAR DEDE

BOGAZICI UNIVERSITY

2009

CLIMATOLOGICAL TRAJECTORY ANALYSIS OF AIR POLLUTION FROM  
ISTANBUL TO ITS SURROUNDINGS

by

Bahar Dede

BS. in Env. E., Trakya University, 2004

Submitted to the Institute of Environmental Sciences in partial fulfillment of

the requirements for the degree of

Master of Science

in

Environmental Technology

Boğaziçi University

2009

CLIMATOLOGICAL TRAJECTORY ANALYSIS OF AIR POLLUTION FROM  
ISTANBUL TO ITS SURROUNDINGS

APPROVED BY:

Prof.Dr. Orhan Yenigün .....

(Thesis Supervisor)

Doç.Dr. Tayfun Kindap .....

(Thesis Supervisor)

Prof.Dr. Ayşen Erdinçler .....

Doç.Dr. Nadim Copty .....

Prof.Dr.Selahattin İncecik .....

DATE OF APPROVAL (18/06/2009)

## ACKNOWLEDGEMENTS

First and foremost, I would like to acknowledge and extend my heartfelt gratitude to my thesis supervisor Prof. Dr. Orhan Yenigün who has supported me throughout my thesis project with his guidance, patience, tenderness and knowledge.

I would like to express my sincere gratitude to my thesis co-supervisor Doç. Dr. Tayfun Kindap for his great deal of interests, encouragement, guidance and support from the initial to the final level enabled me to develop an understanding of the subject. Without his encouragement and constant guidance, I could not have finished this dissertation. His perpetual energy and enthusiasm in research had motivated all his advisees, including me. One simply could not wish for a better or friendlier supervisor.

I would also like to thank Ulaş Im, for his friendship, encouragement and guidance during my research. I am deeply indebted to Alper Ünal from Eurasia Institute of Earth Sciences, Istanbul Technical University. His interest, support, stimulating suggestions and encouragement helped me in all the time of the research.

I am grateful to all people who have helped and inspired me during my thesis study in the Institute of Environmental Sciences, Boğaziçi University and Eurasia Institute of Earth Sciences, Istanbul Technical University.

I offer my regards and blessings to all people who supported me in any respect during the completion of my research.

Last, but not least, I thank my family and close friends for their unflagging love, support and encouragement throughout my life and most importantly, for believing in me. It is to them that I dedicate this work.

## ABSTRACT

Air pollution is the contamination of air by the discharge of harmful substances. Day by day, air pollution is becoming a very serious issue for all over the world including Turkey. Especially, megacities' pollution problems are rising day by day because of population growth, transportation, traffic and industrial activities. In these megacities, there is a relationship between air pollution and adverse health effects.

Istanbul is one of the largest cities in Europe with dense residential and commercial buildings and high traffic volumes. Dense population and vehicle traffic, irregular urbanization and industrialization are the important problems of Istanbul that contribute to the air pollution.

In the first part of this research, trans-boundary pollutant transport originating from Istanbul was assessed in terms of meteorology and trajectory approach. The aim of this study was to show the impact of the air pollution in Istanbul to its surroundings, especially to the other cities in its vicinity. NCEP/NCAR (National Centers for Environmental Predictions/National Centers for Atmospheric Research) reanalysis data (NNRP-NCEP NCAR Reanalysis Project -2.5°, 6-hourly) for the 30-year period from 1961 to 1990 was used for a comprehensive climatological trajectory evaluation.

The second part of the research contains a case study for a selected episode (22- 25 July 2002) using MM5 model. The aim of selecting this period is that; different wind directions were seen in Istanbul and its surroundings.

Results show that, Istanbul is a regional air pollution source for its surroundings. Air pollutant may be transport from Istanbul to the surrounding area throughout the year as a result of the main wind directions. Although climatological trajectory approach gives general knowledge about air transport, it is impossible to predict daily air parcel movements based on it.

## ÖZET

Hava kirliliği, havadaki yabancı maddelerin normalin üzerindeki miktar ve yoğunluğa ulaşmasıdır. Gün geçtikçe, hava kirliliği tüm dünyada olduğu gibi Türkiye için de ciddi bir sorun haline gelmektedir. Hızlı nüfus artışı, ulaşım, trafik, endüstriyel faaliyetler ve düzensiz şehirleşme gibi sebeplerden dolayı, büyük şehirlerin kirlilik problemleri her geçen gün artmaktadır. Bu şehirlerde, hava kirliliği ile artan ölüm oranları arasında ciddi bir ilişki söz konusudur.

İstanbul, yoğun yerleşim alanları ve ticari yapılanması ile Avrupa'nın en büyük şehirlerinden birisidir. Nüfus yoğunluğu, araç trafiği, düzensiz şehirleşme ve endüstriyel faaliyetler, İstanbul'un hava kirliliği artışındaki önemli unsurlardır.

Bu araştırmanın ilk bölümünde, İstanbul kaynaklı uzun mesafeli aerosol taşınımı meteoroloji ve yörünge yaklaşımı ile ele alınmıştır. Çalışmanın amacı, İstanbul'un hava kirliliğinin, çevresine ve özellikle belli başlı büyük şehirlere olan etkisinin ortaya konmasıdır. Kapsamlı bir klimatolojik yörünge modeli yaklaşımı için, 30 yıllık bir periyotta (1961-1990) 2.5° lik çözünürlüğe sahip 6 saatlik NCEP/NCAR Reanalysis verisi kullanılmıştır.

Çalışmanın ikinci kısmında ise, belirli bir episod için (22-25 Temmuz 2002) MM5 modeli çalıştırılarak yörünge tahmini yapılmıştır. Bu tarihlerin seçilmesindeki neden, İstanbul üzerinde etkili olan hakim rüzgarların farklı yönler göstermesidir.

Sonuç olarak, İstanbul'un çevresi açısından önemli bir bölgesel kirlilik kaynağı olduğu tespit edilmiştir. Hava kirleticilerin, tüm yıl boyunca, hakim rüzgarların etkisi ile İstanbul'dan çevresine taşındığı görülmektedir. Her ne kadar klimatolojik yörünge yaklaşımı, kirleticilerin taşınımı hakkında genel bir bilgi verse de, günlük hava hareketlerinin buna bağlı olarak tahmin edilebilmesi mümkün değildir.

## TABLE OF CONTENTS

ACKNOWLEDGEMENTS	iii
ABSTRACT	iv
ÖZET	v
LIST OF TABLES	vii
LIST OF FIGURES	vii
LIST OF SYMBOLS/ABBREVIATIONS	x
1. INTRODUCTION	1
2. BACKGROUND	4
2.1. History of Air Pollution in Cities	4
2.2. Modelling Air Pollution	5
2.3. Study Area: Istanbul	9
3. AIR QUALITY & METEOROLOGICAL EVALUATION	11
3.1. Meteorology of Istanbul	11
3.1.1. Precipitation	14
3.1.2. Temperature	17
3.1.3. Wind	19
3.2. Air Quality in Istanbul	27
3.2.1. Emission	27
3.2.2. Observation	30
4. DATA AND METHODOLOGY	33
4.1. Data	33
4.2. Climatological Trajectory Approach	34
4.3. MM5 Mesoscale Meteorological Model	39
4.3.1. The MM5 Model Horizontal and Vertical Grid	40
4.3.2. Terrain	43
4.3.3. Regrid	46
4.3.4. Interpf	46
4.3.5. MM5	47
5. RESULTS AND DISCUSSIONS	48
5.1. Results of the Climatological Trajectory Approach	48
5.2. A Case Study for a Specific Episode Using MM5	61
6. CONCLUSIONS	66
REFERENCES	68

## LIST OF TABLES

<b>Table 3.1.</b>	General Information for Stations in and around Istanbul.....	12
<b>Table 3.2.</b>	Parameters Measured in Each Station.....	32
<b>Table 4.1.</b>	Description of 24-Category (USGS) Land-Use Categories.....	45
<b>Table 5.1.</b>	Number of Arriviling, Probability of Arrival, and Average Travel Time from Istanbul to Selected Cities.....	50



## LIST OF FIGURES

<b>Figure 2.1.</b>	Distribution of Population Density in Istanbul.....	10
<b>Figure 3.1.</b>	Distribution of Stations and Land-Use Map.....	13
<b>Figure 3.2.</b>	Elevation Map of Istanbul and Topographic Sections.....	13
<b>Figure 3.3.</b>	Average Annual Precipitation Map and Monthly Precipitation Distribution of Some Stations in Istanbul.....	16
<b>Figure 3.4.</b>	Average Annual Temperature Distribution of Istanbul and Monthly Temperature Values of Some Stations.....	18
<b>Figure 3.5.</b>	Distribution of Average Annual Wind Speed in Istanbul.....	19
<b>Figure 3.6.</b>	Wind Directions and Speeds in Winter Months.....	22
<b>Figure 3.7.</b>	Wind Directions and Speeds in Spring Months.....	23
<b>Figure 3.8.</b>	Wind Directions and Speeds in Summer Months.....	24
<b>Figure 3.9.</b>	Wind Directions and Speeds in Autumn Months.....	25
<b>Figure 3.10.</b>	Annually Wind Directions and Speeds.....	26
<b>Figure 3.11.</b>	Population and Number of Vehicles in Istanbul.....	29
<b>Figure 3.12.</b>	Distribution of Air Quality Measurement Stations in Istanbul.....	31
<b>Figure 4.1.</b>	The Construction of Trajectories by Successive Approximations.....	35
<b>Figure 4.2.</b>	Second approximation is obtained by the mean of the two displacement.....	36
<b>Figure 4.3.</b>	The Construction of Trajectories From Streamlines and Isotach Charts.....	37
<b>Figure 4.4.</b>	The MM5 Modeling System Flow Chart.....	39
<b>Figure 4.5.</b>	Schematic Representation of the Vertical Structure of the Model.....	41
<b>Figure 4.6.</b>	Schematic Representation Showing the Horizontal Arakawa B-grid Staggering of the Dot (I) and Cross (x) Grid Points.....	42
<b>Figure 5.1.</b>	Graph of the Number of Arrival Trajectories and the Probability of Arrival (%).....	51
<b>Figure 5.2.</b>	Maps of a) The Air Distribution and b) Average Travel Times From Istanbul to the Selected Cities for Winter Duration (12 <sup>th</sup> , 1 <sup>st</sup> and 2 <sup>nd</sup> Months).....	52
<b>Figure 5.3.</b>	Maps of a) The Air Distribution and b) Average Travel Times From	

	Istanbul to the Selected Cities for Spring Duration (3 <sup>th</sup> , 4 <sup>th</sup> and 5 <sup>th</sup> Months).....	54
<b>Figure 5.4.</b>	Maps of a)The Air Distribution and b) Average Travel Time From Istanbul to the Selected Cities for Summer Duration (6 <sup>th</sup> ,7 <sup>th</sup> and 8 <sup>th</sup> months).....	56
<b>Figure 5.5.</b>	Maps of a) The Air Distribution and b) Average Travel Time From Istanbul to the Selected Cities for Autumn Duration (9 <sup>th</sup> ,10 <sup>th</sup> and 11 <sup>th</sup> months).....	58
<b>Figure 5.6.</b>	Maps of a) The Air Distribution and b) Average Travel Time From Istanbul to the Selected Cities Annually.....	60
<b>Figure 5.7.</b>	MM5 Forward Trajectory Approach for 22 July 2002.....	62
<b>Figure 5.8.</b>	Wind Direction and Sea Level Pressure for 22 July 2002.....	62
<b>Figure 5.9.</b>	MM5 Forward Trajectory Approach for 23 July 2002.....	63
<b>Figure 5.10.</b>	Wind Direction and Sea Level Pressure for 23 July 2002.....	63
<b>Figure 5.11.</b>	MM5 Forward Trajectory Approach for 24 July 2002.....	64
<b>Figure 5.12.</b>	Wind Direction and Sea Level Pressure 24 July 2002.....	64
<b>Figure 5.13.</b>	MM5 Forward Trajectory Approach for 25 July 2002.....	65
<b>Figure 5.14.</b>	Wind Direction and Sea Level Pressure for 25 July 2002.....	65

## LIST OF SYMBOLS/ABBREVIATIONS

AMSL	Above Mean Sea Level
ARL	Air Resources Laboratory
AQM	Air Quality Models
CAMX	Comprehensive Air Quality Model
CMAQ	US/EPA Community Multiscale Air Quality Modeling System
CO	Carbon Monoxide
E	East
EDAS	Eta Data Assimilation System
EIES	Eurasia Institute of Earth Sciences
EMEP	European Monitoring and Evaluation Programme
EPA	Environmental Protection Agency
GAMBIT	Gridded Atmospheric Multi-level Backward Isobaric Trajectories
GDAS	Global Data Assimilation System
GIS	Geographical Information System
HC	Hydrocarbon
HYSPLIT	Hybrid Single-Particle Lagrangian Integrated Trajectory
Lat.	Latitude
Lon.	Longitude
LPG	Liquefied petroleum gas
LSM	Land-surface model
MM5	Fifth-Generation NCAR/Penn State Mesoscale Model
MM5T	MM5 Online Tracer Model
MNPP	Metsamor Nuclear Power Plant
NAT	Number of Arrival Trajectories
NCEP/NCAR	National Centers for Environmental Predictions/National Centers for Atmospheric Research
NE	North-East
NMVOG	Non-methane Volatile Organic Compounds
NNE	North-Northeast

NNRP	NCEP/NCAR Reanalysis Project
NNW	North-Northwest
NOX	Nitrogen oxides
NW	North-West
O <sub>3</sub>	Ozone
PA	Probability of Arrival (%)
PM	Particulate Matter
RIP	Read/Interpolate/Plot
SO <sub>2</sub>	Sulphur dioxide
SOX	Sulphur oxides
SSC	The Spatial Synoptic Classification
SSW	South-Southwest
TUIK	Turkish Statistical Institute
US	United States
USGS	U.S. Geological Survey
W	West

## 1. INTRODUCTION

Air pollution is the presence of substances in the atmosphere, resulting from man-made activities or from natural processes, causing adverse effects to man and the environment. In other words, it is the contamination of air by the discharge of harmful substances. Day by day, air pollution is becoming a very serious issue all over the world including Turkey. Gasses or particulate matters emitted into the atmosphere by human and natural activities cause many current and potential environmental problems, including acidification, air quality degradation, climate change, damage and soiling of buildings and other structures, stratospheric ozone depletion, human and ecosystem exposure to hazardous substances (Jafari et al., 2007). It is important to have quantitative and qualitative knowledge about these emissions, and their sources and distributions to be able to conduct preventive operations.

Air pollution threatens human life. Megacities' pollution problems are rising day by day because of population growth, transportation, traffic and industrial activities. Long-range aerosol transport contributes to the air pollution of cities besides their own pollution sources (Kindap et al., 2006). In these megacities, there is a relationship between air pollution and increased death rate. For that reason, gasses and particulate matters in the air must seriously be investigated.

According to 2008 Address Based Population Registration System, Turkish Statistical Institute, Istanbul is a megacity with nearly 12 millions population (TUIK, 2008). It is the largest cities in Europe with dense residential and commercial buildings and high traffic volumes. Dense population and vehicle traffic, irregular urbanization and industrialization are the important problems of Istanbul that contribute to the air pollution. A limited number of air quality monitoring stations have been established to measure concentrations of air pollutants in Istanbul in real time. Because it is impossible to measure air pollution in every place where it occurs, models are used to simulate the dispersion of air pollutants away from emission sources, and to estimate ground level pollution concentrations. The impacts of air pollution are usually estimated through the use of air

quality simulation models. These models are usually distinguished by type of source, pollutant, transformations and removal, distance of transport, and averaging time. Air pollution modeling is widely used in studying the relationship between air quality, emission sources and meteorology. Air quality models are divided by two types; three-dimensional Eulerian and Lagrangian models (Bultjes, 2001).

A Lagrangian dispersion model mathematically follows particles as they move in the atmosphere and the motion of the particles using a moving frame of reference. Lagrangian modelling is often used to cover longer time periods, up to years (Bultjes, 2001). A Lagrangian model is suitable for examining the dispersion from a single source, which represents a large number of parcels that are advected with the wind field obtained from a meteorological model. Complex chemistry can be represented within each parcel. Lagrangian models can be computationally quite intensive, their accuracy depending on the number of particles released, and they can accommodate chemical sub-models. Atmospheric transport and diffusion are simulated by tracking the movement of large numbers of 'particles' that represent quantities of an air pollutant according to average wind and turbulence parameters with random movement. Both average wind conditions and specifically prescribed flow-fields can be accommodated to control the movement of the particles.

Eulerian model on the other hand uses a fixed three-dimensional Cartesian grid. A Eulerian model is suitable for modelling a situation with many distributed sources, as it carries concentration values at every point on a grid. Due to the much-increased number of points represented, the chemistry is usually much simpler than in a Lagrangian model. A Lagrangian model has the potential advantage in that it may calculate more accurately the advection and dispersion from various sources and allow more complete characterization of the impact of turbulence on the transport of air pollutants. An Eulerian model allows for the treatment of the chemical interactions of all air parcels within a grid square (Gertler, 2006).

Trajectory analyses are commonly used in air quality studies to examine the source regions of air parcels moving into a given area, or the likely paths air parcels would take

following a plume from a point source. In addition to tracking the movement of air parcels, it is also important to consider thermodynamic factors that could influence changes in air quality (Kindap, 2005).

In this study, trans-boundary pollutant transport originating from Istanbul was assessed using a meteorology and trajectory approach. The goal of this study is to present the impact of the air pollution of Istanbul to its surroundings, especially to nearby cities. A period of 30-year (1961-1990) NCEP/NCAR (National Centers for Environmental Predictions/National Centers for Atmospheric Research) reanalysis data (NNRP-NCEP NCAR Reanalysis Project -2.5°, 6-hourly) was used for a comprehensive climatological trajectory evaluation. Generally, air quality models are used to estimate the air pollutant concentration (i.e CMAQ), but emission inventory for the area of interest is difficult to find and running the model is a hard and complex study that requires a long time effort. The advantage of this study is to be able to use NCEP/NCAR reanalysis data for a 30-year-period, it which would be impossible to run an atmospheric dispersion model for the same long period (Kindap, 2005). The second part of this study contains a case study for a selected episode (22- 25 July 2002) using MM5 model. The aim of selecting this period is that; different wind directions were seen on Istanbul and its surroundings. Forward trajectories were generated during this period to be able to see the similarities and differences with the climatological trajectory approach for a 30-year period.

## **2. BACKGROUND**

### **2.1. History of Air Pollution in Cities**

If volcanic ashes, salt particulates from oceans, hydrocarbon and pollens from forests are considered, air has never been clean. With the beginning of the humanity, antropogenic sources have been contributing to air pollution besides natural sources.

In Ancient Rome, it is known that the city had serious air pollution because of the use of wood for heating. In that time in the Mediterranean Region and in China (between 960-1279) copper melting was a significant air pollution source (Hong and Pan, 1996).

In London, coal usage led to an increase in air pollution. In 1285 a comission was founded for this reason. With the impact of this comission, King I. Edward banned the usage of coal in limekilns. Although heavy penalties, even death penalties were imposed, coal was used again in 1309 (Brimblecombe, 1987). Because, wood was used instead of coal and this was damaging to forests. Between 13th and 18th centuries, air pollution had risen through coal usage (Jacobson et al., 2005).

In the 18th century, air pollution had gone from bad to worse with the invention of the steam engine in England. Unfortunately, between 1800-1900, deaths from air pollution were seen in the country (Clapp, 1994).

Air pollution has become a very important problem for many big cities since the industrial revolution. For example; in Belgium, in December, 1930; pollutants stayed on Meuse Valley for 5 days and this caused the death of 63 people and the illness of almost 6000 people. This is the first air pollution event which was researched in detail. In October, 1948; thousands of people became ill and 20 persons died because of air pollution, in Donor, Pennsylvania. One of the most terrible air pollution events was experienced in London, in December,1952. After a five-day-pollution, more than 4000 people died.



Especially elderly people were faced with respiration and heart problems. Abnormal air pollution events were seen in London (in 1953 and 1962) and in New York (in 1953, 1963 and 1966) (Jacobson, 2002).

These events show the significance of the air pollution problem, and lead to the development of air quality standards, mitigation measures and scientific methods to accurately quantify the problem.

## **2.2. Modelling Air Pollution**

Forward and backward trajectory models are used to show the pathway of an air parcel. Forward trajectories are drawn from the point of selected source to where the air parcel might arrive. Back trajectories show the pathway of air parcel from the end point to the possible source it might come from (Innocentini, 1999).

Forward trajectory approach is used for the Mt. Etna Plume by Martin et al. (1984). Trajectories are computed for a 3-day period (at 700 mb) using 18-year meteorological data (1963-1980). After 3 day, trajectory determinations present a high degree of uncertainty and become too much dispersed towards the geographical location of their arrival point. Significant differences between seasonal typical trajectories are emphasized. It is shown that the plume can reach more than 2000 km especially during the summer (Martin et al., 1984).

“Climatology of Back Trajectories from Israel Based on Synoptic Analysis” is a backward trajectory approach studied by Dayan, 1986. The research summarizes five years of back trajectories calculated by using the GAMBIT (Gridded Atmospheric Multi-level Backward Isobaric Trajectories) (Harris, 1982) of ARL (Air Resources Laboratory). Trajectories are generated for the Eastern Mediterranean Basin at 850 mb using five years of data from January 1978 to December 1982 (Harris, 1982). The flow transport is mostly from Northwestern Europe along the Mediterranean Area during the winter period. Secondary flow transport is mainly from Eastern Europe (Dayan, 1986).

McGowan et al. (2005) studied high resolution provenancing of long travelled dust deposited on the Southern Alps, New Zealand. On 7 February 2000 a typical orange discolouration of snowfields in the central Southern Alps, New Zealand occurred following the passage of a cold front. To determine the areas affected by dust storms atmospheric transport pathways from areas affected by dust storms on 4 February, forward air parcel trajectories were computed using the HYSPLIT\_4 (HYbrid Single-Particle Lagrangian Integrated Trajectory) model (Draxler and Hess, 1998). This model uses NCEP (National Centers for Environmental Prediction) 6 hourly reanalysis data to compute the trajectory (either forward or backward) of a particle through the atmosphere, and is therefore well suited to the study of long distance atmospheric transport of dust. Importantly, it allows the transport trajectory of dust plumes to be studied in regions where no observational data exist. This study showed the potential for transport of dust from Lake Eyre to the Antarctic and much of the South Pacific and Southern Oceans (McGowan et al., 2005).

Kindap et al. (2006) investigated long-range aerosol transport from Europe to Istanbul using backward trajectory analysis. They ran Fifth-Generation NCAR/Penn State Mesoscale Model (MM5) to generate meteorological data and the emissions processor to generate emission data (Grell et al., 1994). Then this data were input to US/EPA Community Multiscale Air Quality Modeling System (CMAQ) to perform pollutant transport and chemical transformation, to simulate a winter episode in Europe. The National Centers for Environmental Prediction (NCEP) Global Data Assimilation System (GDAS) data (with  $2.5^\circ \times 2.5^\circ$  resolution) were used for MM5 boundary and initial conditions. MM5 results were used to calculate backward trajectories to understand where pollutants might be coming from. Trajectory analysis shows that Istanbul are affected from especially Eastern European countries by northwesterly winds. As a result, when air pollution of Western and Northern Turkey is considered, the contribution of European countries can be responsible for as much as half of the Istanbul background PM10 levels under certain meteorological conditions (Kindap et al., 2006).

Freiwan and İncecik (2006) investigated European air pollutants transport to the Eastern Mediterranean region. Transport was investigated during the episodic period 26 – 29 August 1998. Meso-scale Meteorological Model, MM5 was applied to forecast the

hourly general circulation conditions and hourly meteorological variables. Air mass backward trajectory simulations were also predicted by MM5/RIP (Read/Interpolate/Plot) and HYSPLIT models. Consequently, three main sectors of air mass trajectory originated from Europe were found. MM5 model outputs were used in the three-dimensional Eulerian photochemical model CAMx to simulate the concentration deposition and the long range transport of the air pollution species such as SO<sub>2</sub>. CAMx air quality model simulations have revealed a great agreement with the air mass trajectory simulations produced by HYSPLIT and RIP/MM5 models and have demonstrated that sulfate transport from central and southeastern Europe to the eastern Mediterranean has two distinguished paths. The modeling system which is used for the first time in Turkey exhibited a high performance (Freiwan and İncecik, 2006).

In another study, back-trajectory and air mass climatology were used for the Shenandoah Valley by Davis et al. (2007). They apply a commonly-used trajectory model (the HYbrid Single-Particle Lagrangian Integrated Trajectory (HYSPLIT) model) and an increasingly popular air mass-based classification (the Spatial Synoptic Classification (SSC)) to characterize daily winter climate variability in Roanoke, Virginia. To run the HYSPLIT model, the Eta Data Assimilation System (EDAS) at 80 km resolution for the period 01.01.1997 – 30.04.2004 is used. 500 m elevation is selected for this study. The SSC requires multiple daily records of a variety of variables measured at the surface, including temperature, dew point temperature, wind, sea-level pressure, and cloud cover (total fraction). For Roanoke, these data are available hourly from 1949–2005. Results indicate very strong consistency between the trajectory and air mass-based approaches, even without considering the impacts of day-to-day evolution of air masses at the terminal station (Davis et al., 2007).

Another study for the influence of long-range transport was demonstrated by Borge et al. (2007). A two-stage clustering methodology was developed and applied to 4-day back trajectories arriving in Athens, Madrid and Birmingham, which experience large, moderate and small numbers of daily PM<sub>10</sub> episodes, respectively. Back trajectories were computed using the Hybrid Single-Particle Lagrangian Integrated Trajectory (HYSPLIT) model for a 3-year period. NCEP/NCAR reanalysis meteorological data were used in this

application. Trajectories arriving at 750, 1500 and 3000 m AMSL (above mean sea level) on each day (12:00 UTC) during the period 2001-2003 were computed. Results suggested that long-range transport from North Africa and continental Europe have a significant impact on PM<sub>10</sub> levels in Madrid and Birmingham, respectively. On the other hand, Athens is moderately affected by particle transport from North Africa, because strong local sources tend to mask long-range transport influences (Borge et al., 2007).

Trans-boundary transport of air pollutants to Istanbul was studied in terms of meteorology, trajectory, tracer and air quality model approach by Kindap et al. (2008). A framework was prepared to model air quality using MM5 for meteorological modeling and CMAQ for transport and chemistry modeling. Based on Fifth-Generation NCAR/Penn State Mesoscale Model (MM5), an online tracer model (MM5T) was used to generate pollutant transport. The National Centers for Environmental Prediction (NCEP) Global Data Assimilation System (GDAS) data (with 2.5° \*2.5° resolution) were used for MM5T boundary and initial conditions. Studies were carried out for two high-pollution events occurred in Istanbul, Turkey on 7-8 and 10-11 January 2002. Backward trajectory approach showed the same geographic location of origin for two high pollution events over the city. As a result, it can be said that transport of pollutants from Eastern European metropolitan cities might contribute to high-pollutant events over the city (Kindap, 2008).

Kindap et al. (2008) emphasized the potential threats from a likely nuclear power plant accident using a climatological trajectory and tracer analysis. First, a 10-day trajectory analysis was carried out with a 30-year meteorological data. Second, a tracer study was performed using the MM5T online model. Forward trajectory and tracer analysis showed that an accident at the Metsamor Nuclear Power Plant would affect all of Turkey. A 30-year period The National Centers for Environmental Prediction/National Centers for Atmospheric Research (NCEP7NCAR) reanalysis data (with 2.5° \*2.5° resolution, 6 hourly) was used for the climatological trajectory approach ( $\sigma = 0.995$ , near surface level). The study showed that besides the northern part of Turkey, other parts (Marmara Region, the Aegean Region and even the Central Anatolian Region) were influenced by the Chernobyl accident. It was demonstrated that if there had been an accident at the Metsamor Nuclear Power Plant (MNPP) on April 26, 1986 instead of Chernobyl, Turkish territory,

especially the Eastern part, would have faced an extremely serious problem which would not be able to recover for many years (Kindap et al., 2008).

### **2.3. Study Area: Istanbul**

Istanbul is the biggest city in Turkey with more than 12 million populations according to 2008 Address Based Population Registration System, Turkish Statistical Institute, (TUIK, 2008). The city is located in the north-west of the country. The Bosphorus, a seawater strait extending from Black Sea to Marmara Sea, divides the city into the European and the Anatolian parts. Istanbul encloses the southern Bosphorus which places the city on two continents—the western portion of Istanbul is in Europe, while the eastern portion is in Asia.

Within the last 40 years, the city has experienced a rapid growth in urbanization and industrialization. Statistics show that the population of the city is over 10 million, more than 2 million motor vehicles registered in Istanbul and about 400 new cars are added to the city traffic everyday (TUIK, 2008, EIES, 2005).

The counties which have great population density (more than 15.000 person/ square kilometres) are, respectively: Fatih, Bayrampaşa, Güngören, Esenler, Bahçelievler, Beyoğlu, Kadıköy, Üsküdar, Ümraniye, Beşiktaş, Kâğıthane, Zeytinburnu, Bakırköy and Küçükçekmece (EIES, 2005) as seen in Fig. 2.1.

Migration to Istanbul contribute to the rise in pollution sources. Irregular urbanization reduced green areas and high buildings affect air circulation. Especially, high buildings along the coast prevent breezes that can distribute the pollutants.

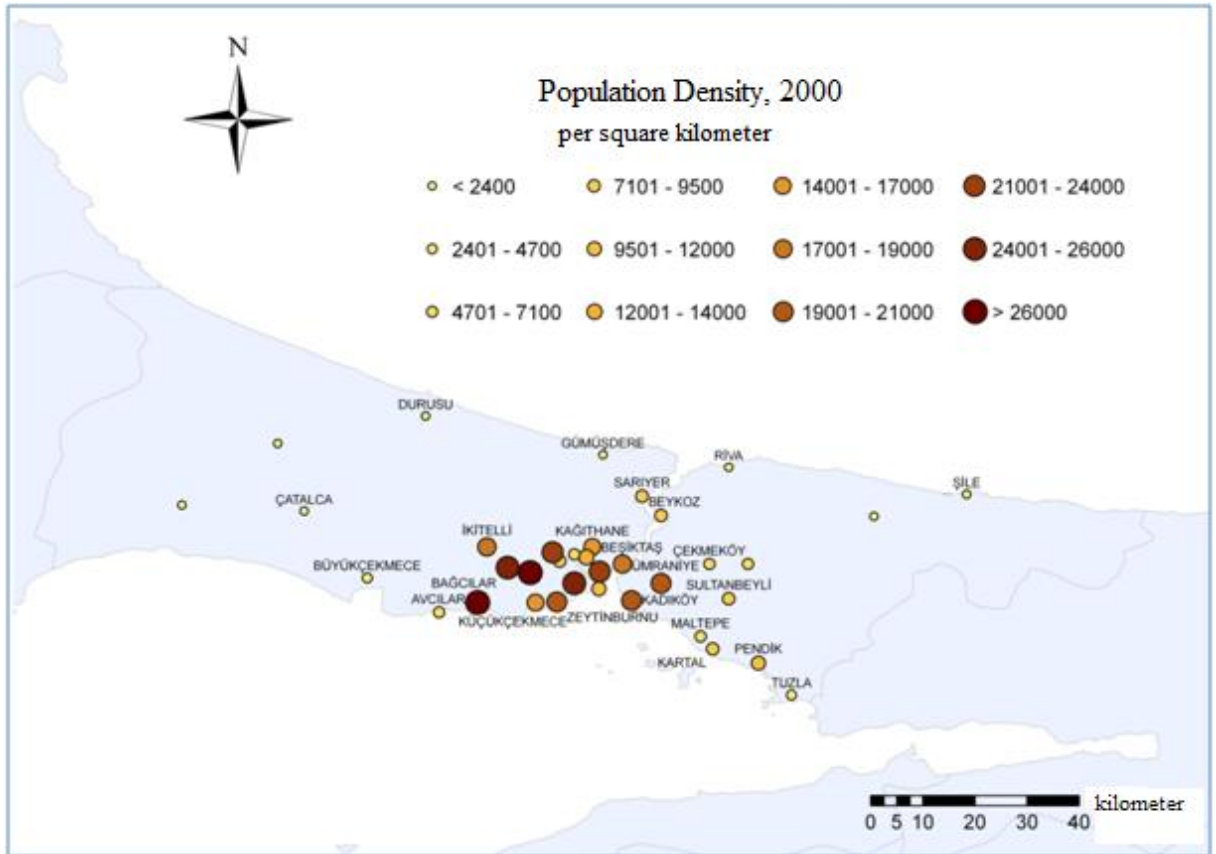


**Figure 2.1.** According to the Population Census in 2000, Distribution of Population Density in Istanbul (EIES, 2005).

### 3. AIR QUALITY & METEOROLOGICAL EVALUATION

#### 3.1. Meteorology of Istanbul

The city of Istanbul, located at 41.01°N, 28.58 °E, is the largest city in Turkey with a population of over 12 million (TUIK, 2008). The Bosphorus, a 30-km strait that connects the Black Sea with the Sea of Marmara, is considered to be the boundary between Europe and Asia, and urban Istanbul is located on both sides of the southern half of the strait. Istanbul region –due to its position- has both Black Sea Climate and Mediterranean Climate. Mediterranean Climate, comes throughout Aegean and Marmara Sea (Ezber et al., 2007).

Table 3.1. shows meteorological stations in Istanbul and its vicinity. Bold ones are around Istanbul.

The location of 12 stations in Istanbul are shown in Fig. 3.1. with land use types including agricultural areas, forests , urban and wetlands. As it is seen on the map; Florya, Göztepe, Kartal, Kandilli and Kireçburnu Stations are urban, Karacaköy, Bahçeköy, Ömerli, Teke, Şile and Kumköy Stations are suburban and rural areas, Çatalca Station is in agricultural area. Most of them are positioned along the Bosphorus and the Marmara Sea that are densely urbanized (EIES, 2005).

Göztepe is an urban station, completely engulfed by dense city buildings and structures. Florya is also an urban station, but it is open to direct sea effect from the south. Kandilli and Kireçburnu are suburban stations and both are located on the hills overlooking the Bosphorus. Kandilli, however, is closer to the densely urbanized areas compared to Kireçburnu. Bahçeköy is an inland rural station surrounded by forest areas, and Kumköy is a rural station in an area on the Black Sea coast that has only been recently subject to urbanization. The elevations of the stations are within 150 m from the mean sea level and the differences between the elevations of these stations are not more than 100 m (Ezber et al., 2007).

**Table 3.1.** General Information for Stations in and around Istanbul (Istanbul Climate and Air Pollution Report, EIES, 2005).

Station Name	Latitude	Longitude	Height(m)	Data Length (year)
ÇORLU	41.17	27.8	183	69
TEKİRDAĞ	40.98	27.55	4	74
SARAY	41.44	27.92	152	5
KIRKLARELİ	41.73	27.23	232	75
MARMARA EREĞLİSİ	40.97	27.96	5	5
LÜLEBURGAZ	41.40	27.35	46	73
YALOVA	40.65	29.27	4	63
KOCAELİ	40.78	29.93	76	73
KANDIRA	41.07	30.15	154	11
ÇINARCIK	40.65	29.12	20	37
GEBZE	40.80	29.43	157	9
ŞİLE	41.18	29.61	31	66
FLORYA	40.98	28.75	36	69
KARTAL	40.90	29.18	28	55
GÖZTEPE	40.97	29.08	33	76
BAHÇEKÖY	41.17	28.94	130	58
KUMKÖY	41.25	29.03	30	54
KANDİLLİ	41.05	29.06	115	92
ÇATALCA	41.14	28.47	29	10
ÖMERLİ	41.08	29.33	22	4
KİREÇBURNU	41.17	29.04	58	57
KARACAKOY	41.41	28.39	16	5
TEKE	41.07	29.66	99	8



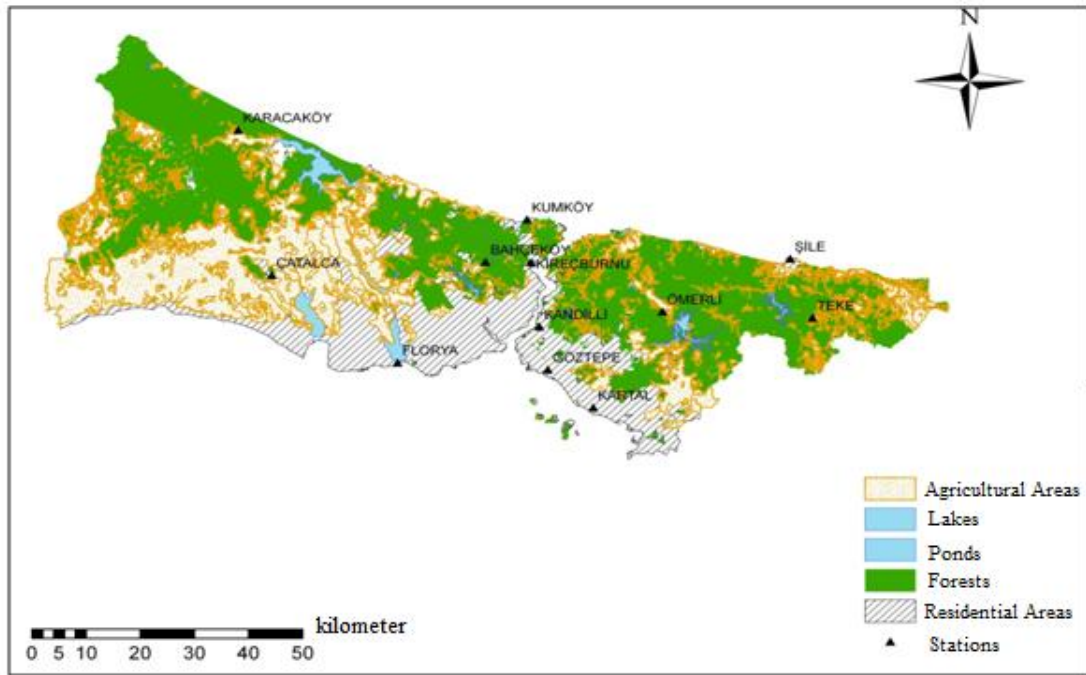


**Figure 3.1.** Distribution of Stations and Land-Use Map (Istanbul Climate and Air Pollution Report, EIES, 2005)

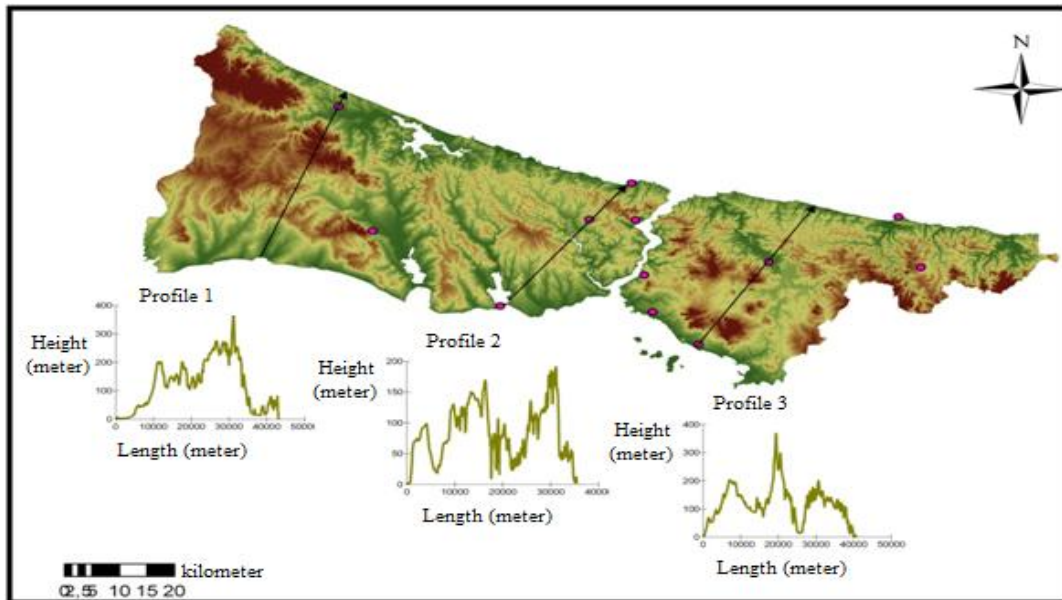


**Figure 3.2.** Elevation Map of Istanbul and Topographic Sections (EIES, 2005)

In Fig. 3.2., elevation map (at 50 m resolution) for Istanbul and section of elevations pass from some stations. Generally, Istanbul is not very high from sea-level (a few hundreds of meters). So, elevation is not an distinctive issue in terms of climate.

The southern parts of provincial Istanbul, where urban areas mostly lie, show the general characteristics of the Mediterranean climate. However, as one goes northward, the Mediterranean type climate is somewhat modified by the cooler Black Sea and northerly colder air masses of maritime and continental origins. This type is locally called ‘the Black Sea Climate’ and described as having cooler temperatures in both winter and summer, and usually experiences more precipitation compared to the climate of the Mediterranean coasts of Turkey. The northern parts of Istanbul, thus, have slightly cooler temperatures compared to the south. While the south receives about 650 mm precipitation per year, the inland parts receive about 1050 mm and the northern (the Black Sea) coasts about 850 mm annual precipitation. Istanbul, based on station averages, has average air temperatures of 28°C in summer and 8°C in winter. Average annual total precipitation is around 850 mm. The city is subject to moisture laden mid-latitude cyclones during winter months (Kindap, 2008); thus most of the precipitation falls in winter. Summer months have the lowest rainfall amounts. The prevailing wind in Istanbul is northeasterly; but southwesterly winds are also effective during a considerable part of the year. On the basis of the station measurements during the last 30 years, average annual wind speed is  $2.72 \text{ ms}^{-1}$ . Average seasonal wind speed is highest in winter ( $2.97 \text{ ms}^{-1}$ ) and lowest in summer ( $2.39 \text{ ms}^{-1}$ ) (Ezber et al., 2007).

### **3.1.1. Precipitation**

Average annual precipitation is around 630 mm in Turkey. Black and Mediterranean coastal regions (around 1000 mm) receive more precipitation than midlands (around 300 mm) of Turkey. This situation is the result of mountains’ parallel positions to the coasts. Humid air comes from the sea and rise up in the mountains. Because of the generation of cooling, moisture condensate and precipitation occurs. In conclusion; air arrives at the mid areas with less humidity, so precipitation in midlands are not as much as in seashores. The situation is a little different in the Marmara and the Aegean Regions. Elevation is less than other regions and mountains are perpendicular to the Aegean Coastline, so humid air can

travel to mid regions. Precipitations dwindle gradually from seaside to mid areas (EIES, 2005).

Istanbul's geographical position is very different from other cities. It is a band of land, between the Black and the Marmara Sea, with a 30 km-width. Elevation is small. According to the stations in Istanbul, average annual precipitation is around 850 mm. This is 220 mm higher than the country average. For Istanbul, average annual precipitation map and monthly precipitation distribution of some stations are shown in Fig.3.3. As it was said before, inadequate stations can cause some errors in precipitations distributions (EIES, 2005).

Precipitations generally increase from south to east and from seashores to mid areas. Highest levels are recorded in Bahçeköy, Ömerli and Teke Stations. Average of these 3 stations is around 1097 mm. Precipitations in the stations at the Marmara Coast (Kartal, Göztepe and Çatalca) are generally low (about 665 mm). Average in Black Sea Coast (Şile, Kumköy and Karacaköy) is 864 mm and average in Bosphorus Region (Kireçburnu and Kandilli) is 846 mm. So, Bosphorus and Black Seashores have similar precipitation regimes. As a result, it can be said that there are 3 different precipitation regimes in Istanbul due to its geographical position (between two seas), forests in mid areas and etc., (EIES, 2005).

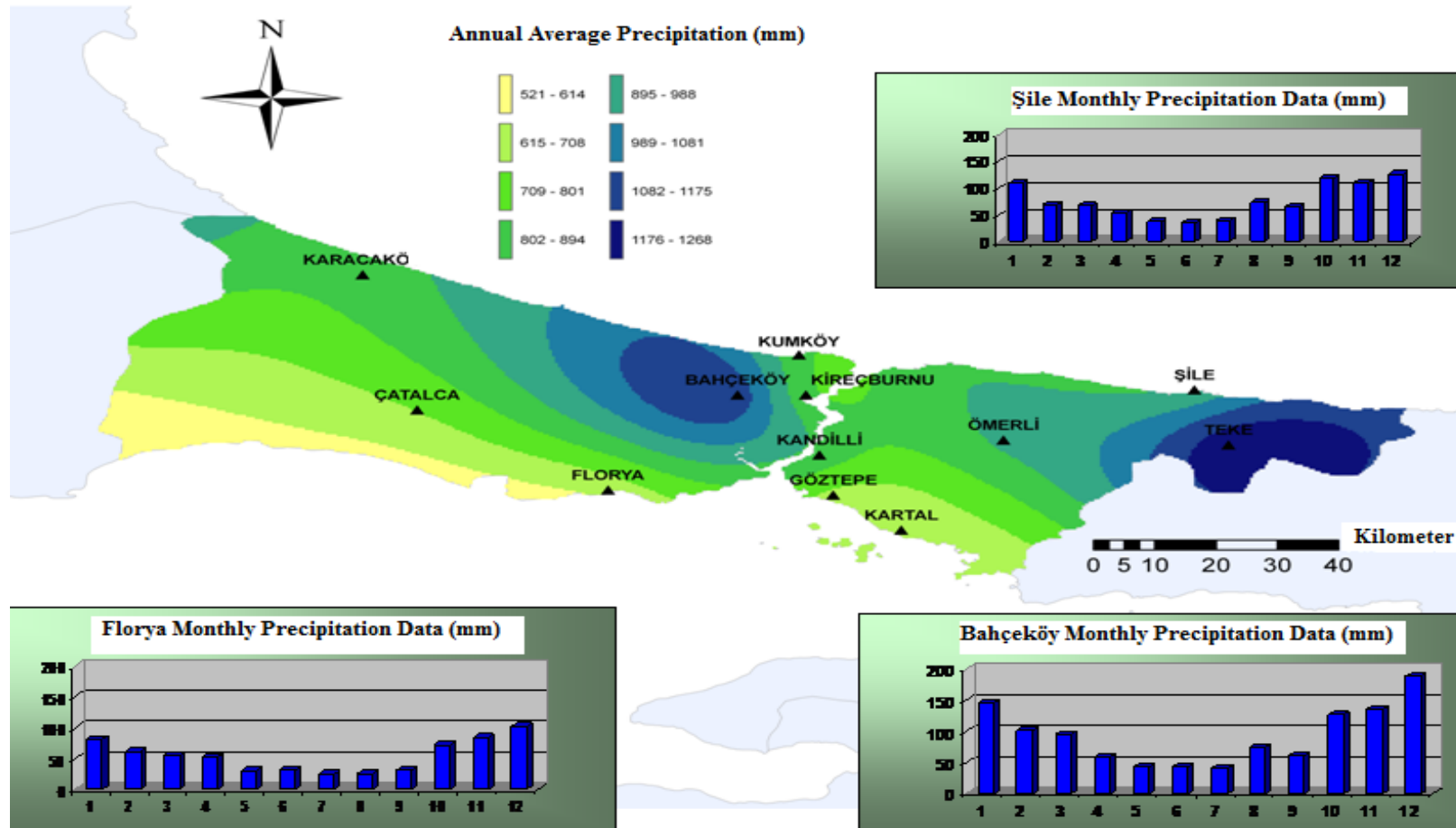
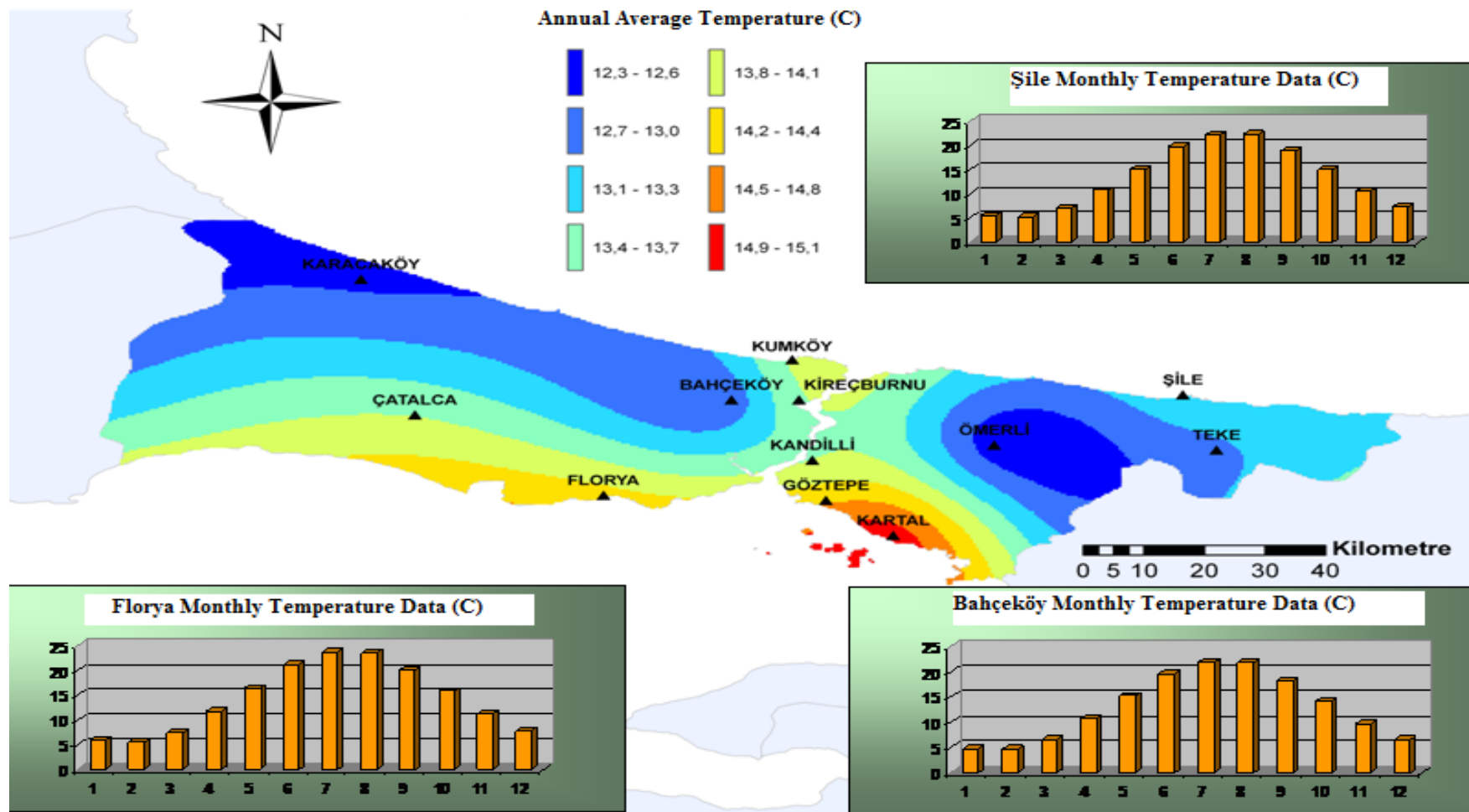


Figure 3.3. Average Annual Precipitation Map and Monthly Precipitation Distribution of Some Stations in Istanbul (EIES, 2005)

### 3.1.2. Temperature

Istanbul has Black Sea climate characteristics more than Mediterranean climate in terms of temperature. Annual average temperature distribution of Istanbul and monthly temperature values of some stations are shown in Fig. 3.4.

There are no large temperature differences between stations. The difference between ones which have the highest and lowest temperature values is only 2.4°C. Temperature decreases gradually from Marmara to Black coastlines and from Bosphorus to mid areas. Highest temperature values were measured at Kartal and lowest values were measured at Ömerli stations. Temperature difference between these two stations is 1.8°C in winter and 3.3°C in the summer period. The Anatolian part of the city is warmer than European part in winters (EIES, 2005).



**Figure 3.4.** Annual Average Temperature Distribution of Istanbul and Monthly Temperature Values of Some Stations (EIES, 2005)

### 3.1.3. Wind

Wind is the most important parameter for air pollution dispersion. Wind direction is the direction from which the wind blows, a west wind would cause pollution to move towards the east from source. Air pollutant concentrations from point sources are probably more sensitive to wind direction than any other parameter. If the wind is blowing directly toward a receptor, a shift in direction of as little as  $5^\circ$  (the approximate accuracy of a wind direction measurement) causes concentrations at the receptor to drop about 10% under unstable conditions, about 50% under neutral conditions, and about 90 % under stable conditions. The direction of plume transport is very important in source impact assessment where there are sensitive receptors or two or more sources, and in trying to assess the performance of a model through comparison of measured air quality with model estimates (Vallero, 2008).

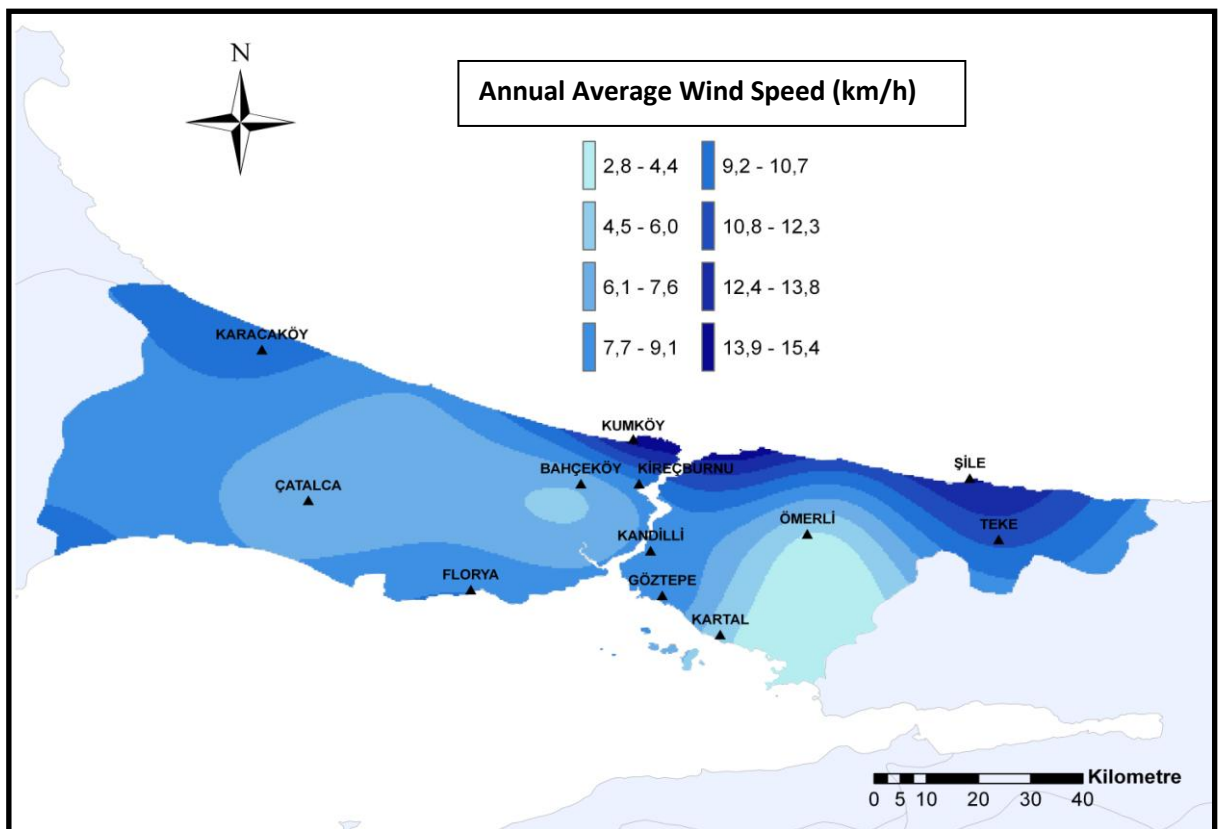


**Figure 3.5.** Distribution of Average Annual Wind Speed in Istanbul (EIES, 2005)

Analysis of wind is rather difficult because its characteristics change with location and elevation. As it can be seen in Fig. 3.5., average annual wind speed is generally high on the Black Sea coastline (Kumköy and Şile stations) and low in mid parts and the east of Kartal station. Along the Bosphorus wind blows faster than in the midlands.

Seasonal distribution of wind parameters are shown in Fig. 3.6-9. Wind roses were only prepared for stations with long measurement periods.

In mid parts, wind speed decreases with the impact of surface friction. Along Bosphorus and Black Sea Coastline, wind speed is high in the main directions.

Fig.3.6. shows the wind directions and speeds taken from stations in Istanbul, for the winter months. In the winter period, the main wind direction is North-Northeast (NNE) for Florya, Göztepe and Kireçburnu, South-Southwest (SSW) for Kumköy and Şile, Northwest (NW) for Bahçeköy and West (W) for Kartal. According to the winter average, forceful winds blow from North-Northwest (NNW) at Kumköy. It can be said that, in the west part of Turkey, northeast wind (with the impact of high pressure region in East Europe) is effective in winter duration. Highest winds were observed in Kumköy Station.

Fig.3.7. shows the wind directions and speeds taken from stations in Istanbul, for the spring months. In March, April and May; winds blow mostly from North-Northeast (NNE) at Şile, Kireçburnu, Göztepe and Florya, from North-Northwest (NNW) at Kumköy, from West (W) at Kartal and from Northeast (NE) at Bahçeköy. Like the winter period, Northeast wind is predominant. Highest winds are observed in Kumköy Station.

Fig.3.8. shows the wind directions and speeds taken from stations in Istanbul, for the summer months. In the summer, except Bahçeköy (NE) and Kartal (E), main wind direction is North-Northeast (NNE). Main wind directions are same in autumn and summer. In addition, highest winds are observed in Kumköy Station.



Fig.3.9. shows the wind directions and speeds taken from stations in Istanbul, for the autumn months. Main wind directions are same in autumn and summer. In Kumköy, Florya, Göztepe, Kireçburnu and Şile, main wind direction is NNE. In Bahçeköy, it is NE. Kartal is different from other stations in terms of main wind direction. In Kartal, mainly easternly (E) and westernly (W) winds were recorded. In addition, highest winds are observed in Kumköy Station.

Fig.3.10. shows the wind directions and speeds taken from stations in Istanbul, annually. In the diagrams (wind roses), frequency (%) and speed (m/sec) for all stations are shown. Generally, main wind of Istanbul is north easterly called the northeast wind. Main wind direction in Şile, Kumköy, Kireçburnu, Göztepe and Florya stations is North-Northeast (NNE), Northeast (NE) in Bahçeköy, west (W) in Kartal, Ömerli and Teke, Northwest (NW) in Karacaköy and North (N) in Çatalca. Highest annual wind speed value (more than 5 m/sec) was recorded in Kumköy from North-North West and South-South West.

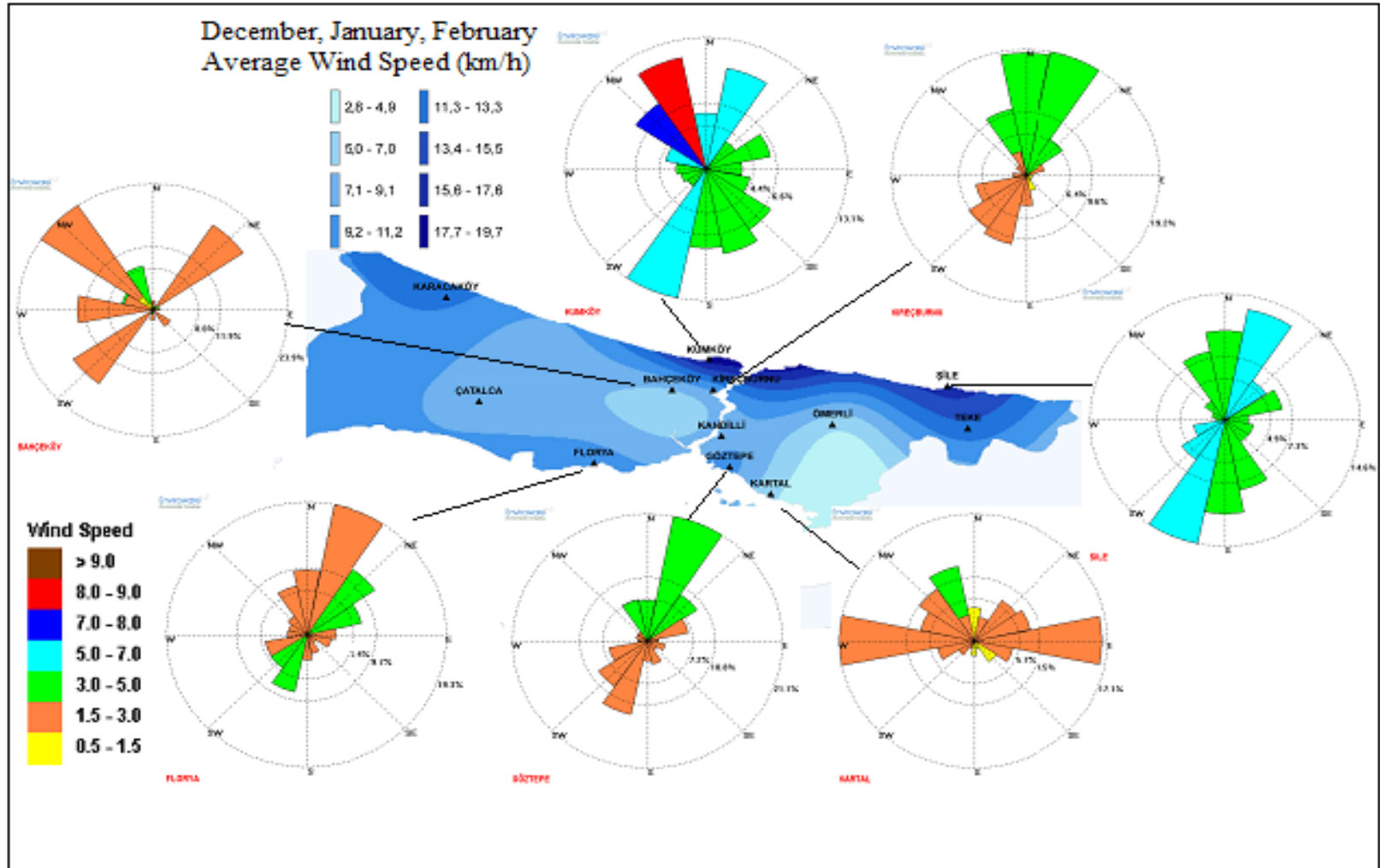
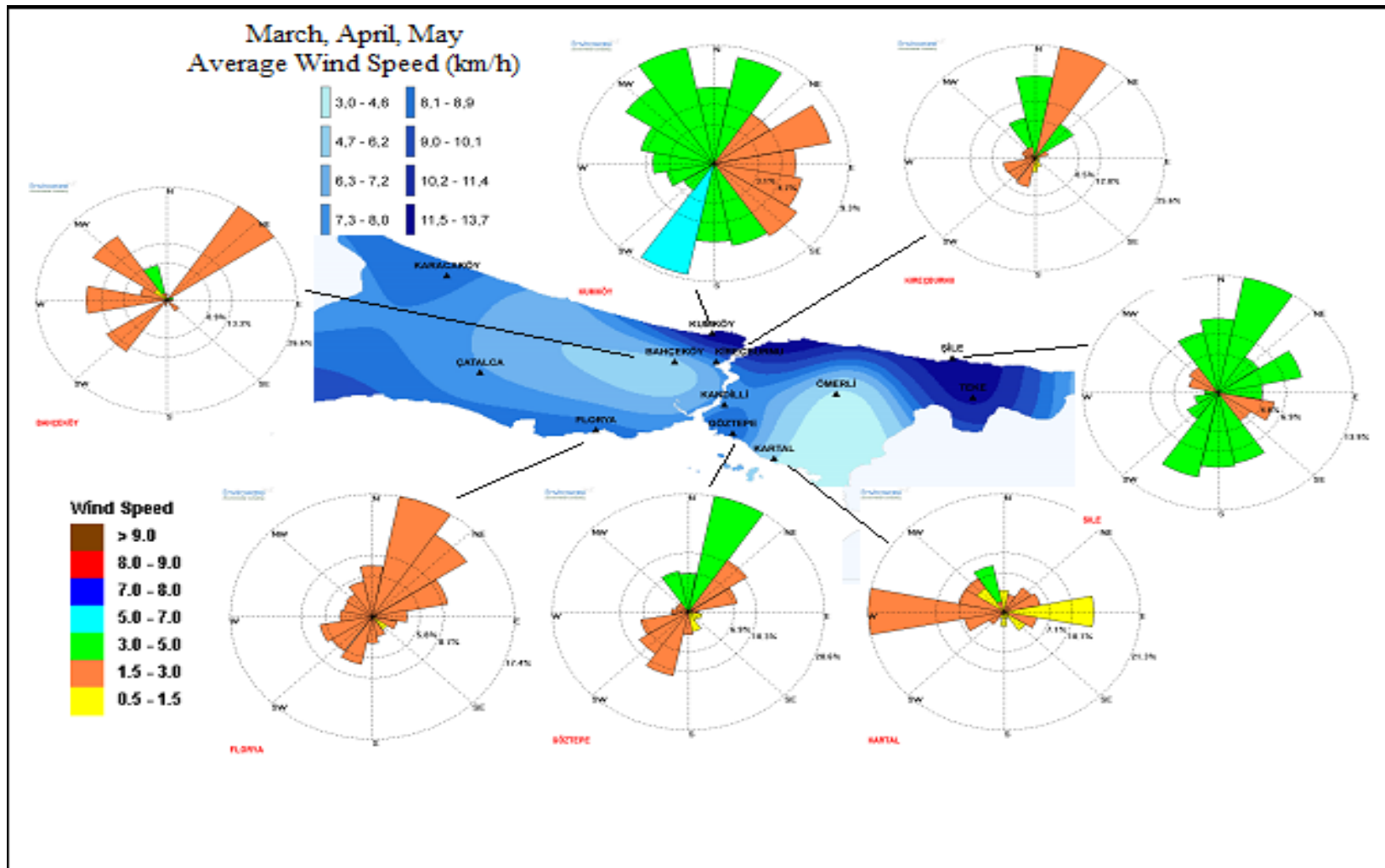
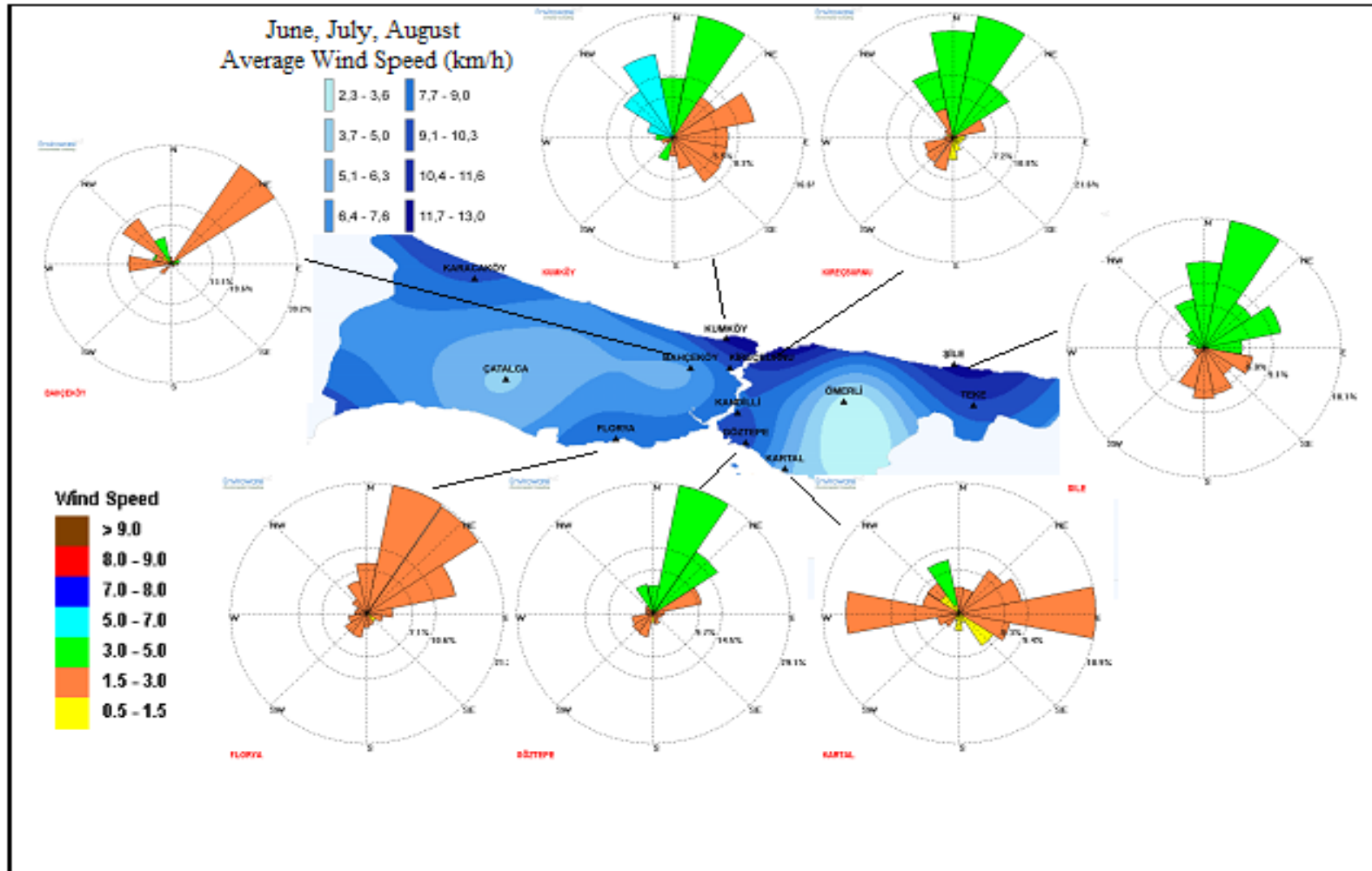


Figure 3.6. Wind Directions and Speeds in Winter Months (EIES, 2005)



**Figure 3.7.** Wind Directions and Speeds in Spring Months (EIES, 2005)



**Figure 3.8.** Wind Directions and Speeds in Summer Months (EIES, 2005)

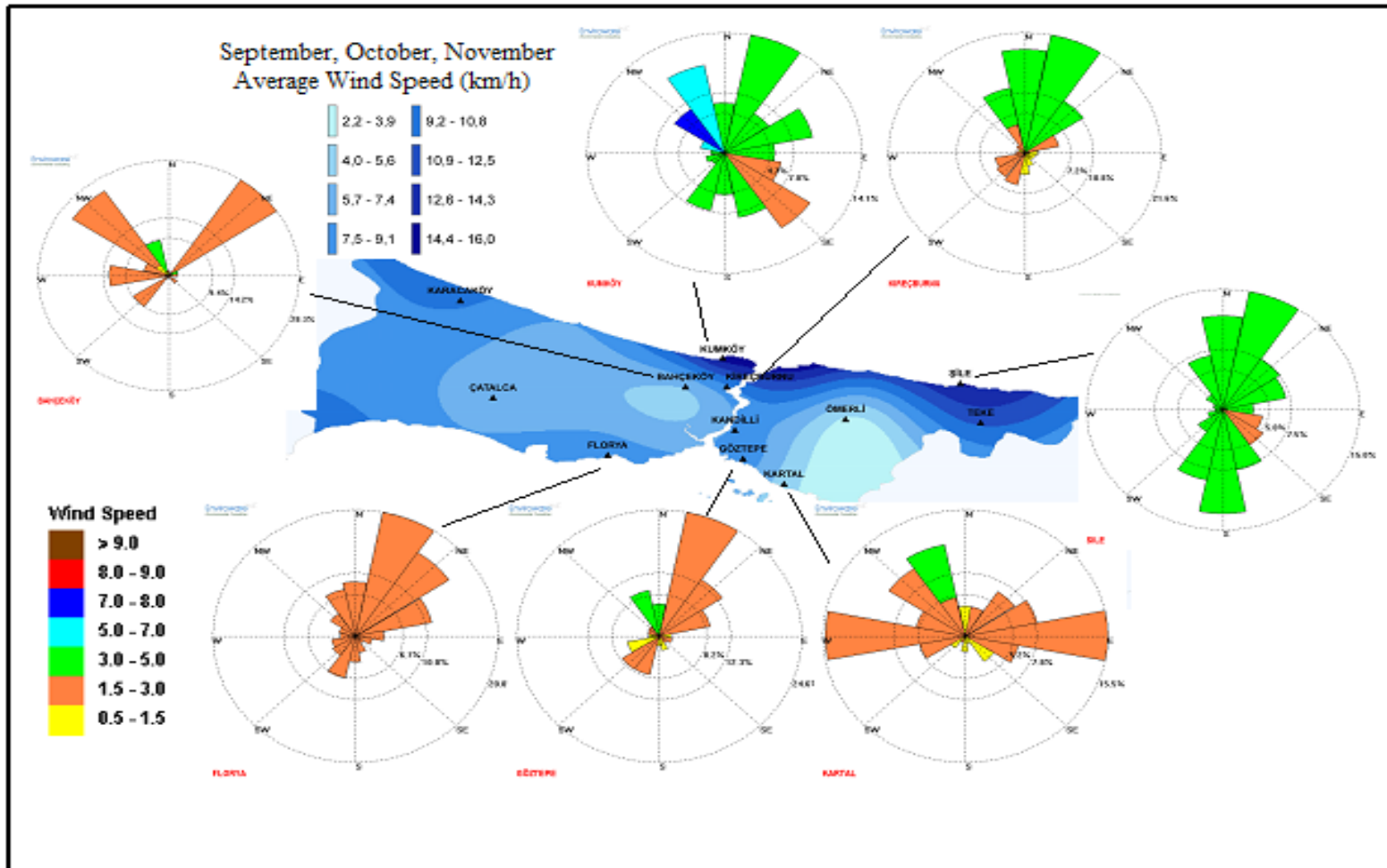


Figure 3.9. Wind Directions and Speeds in Autumn Months (EIES, 2005)

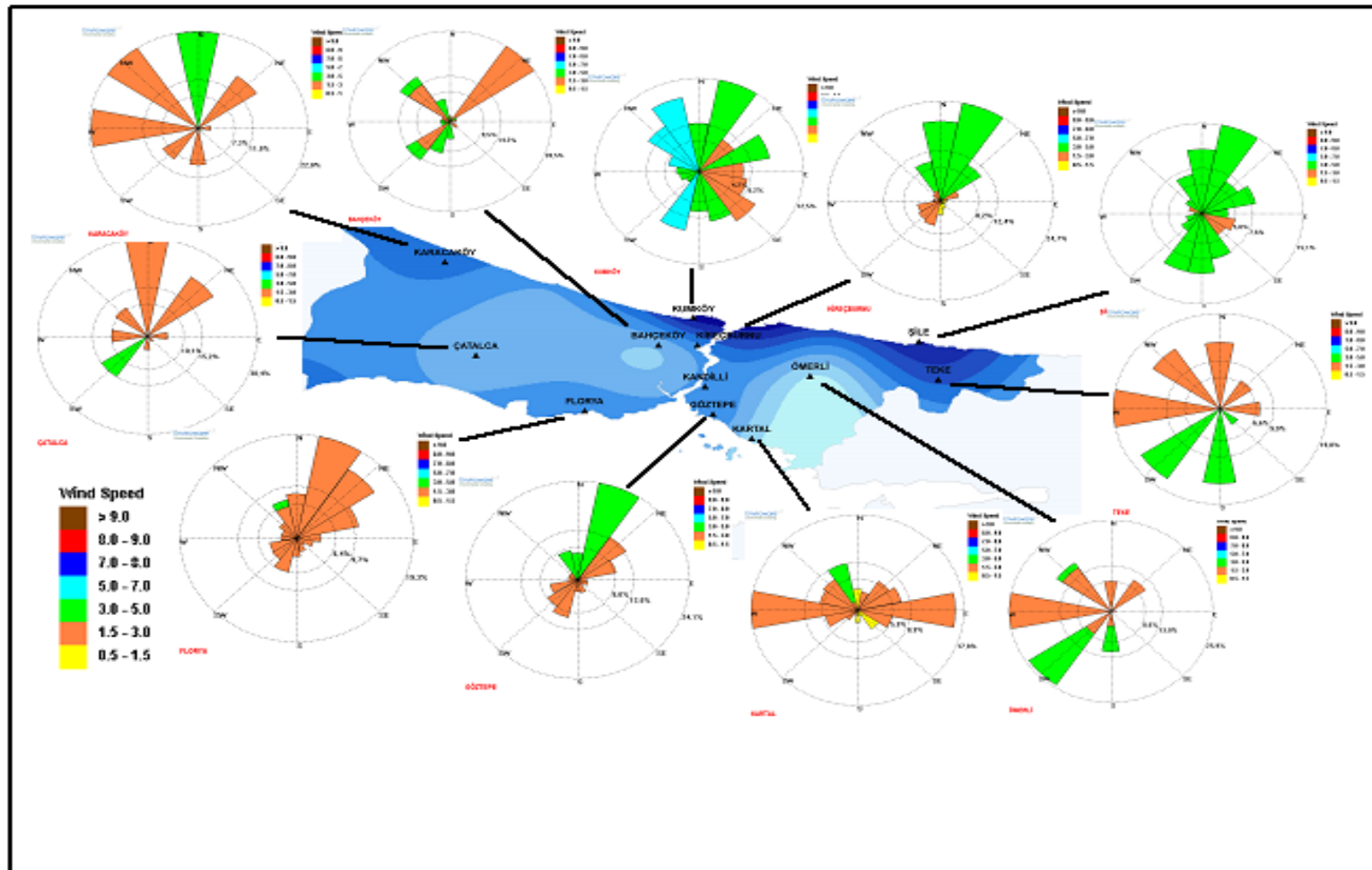


Figure 3.10. Annually Wind Directions and Speeds (EIES, 2005)

## **3.2. Air Quality in Istanbul**

Air pollution moves across national borders. Air pollution of one country influence the others, so Turkey and Europe are affected from each other's pollution. Because of its inevitable effects on human health and significant role in climate change, air quality has become an important issue in societies. These effects can reach vital levels in the megacities of the world. These intensively inhabited areas suffer from rapid urbanization and vanishing green belts because of the requirements of the huge populations. With a population of more than 12 million people and uncontrolled urbanization, the city of Istanbul is one of the most popular examples for this type of the urban settlements (Kindap, 2008).

### **3.2.1. Emission**

Emission is the release of pollutants into the air from a source. Before discussing pollutant emissions of Istanbul, it is necessary to discuss air pollutant emission sources in general. The types of emission sources are commonly characterized as either point, line, area or volume sources (Beychok, 2005).

A point source is a single, identifiable source of pollutant emissions. For example, a combustion furnace flue gas stack is a point source. Point sources have no geometric dimensions and they are characterized as being elevated or at ground-level. Power plants and factories (i.e. cement plants) are important point sources. Line source is one-dimensional source of air pollutant emissions. Vehicular traffic on a roadway is a good example of line source. Area source is a two dimensional source of pollutants like forest fire and landfill. A volume source is a three-dimensional source of diffuse air pollutant emissions. Essentially, it is an area source with a third (height) dimension (for example, the fugitive gaseous emissions from piping flanges, valves and other equipment at various heights within industrial facilities such as oil refineries and petrochemical plants). Another example would be the emissions from an automobile paint shop with multiple roof vents or multiple open windows. Sources may be characterized as either stationary or mobile. Flue gas stacks are examples of stationary sources and buses are examples of mobile sources.

Sources may be characterized as either urban or rural. Urban areas constitute a so-called heat island and the heat rising from an urban area causes the atmosphere above an urban area to be more turbulent than the atmosphere above a rural area (Beychok, 2005; Kostandinou et al., 2009).

Important emission sources in Istanbul are: The energy sector, industrial combustion, industrial processes, residential central heating, extraction and distribution of solid fuels, solvents use, road transport, off-road machinery, cargo shipping, local sea buses/ferries, waste treatment and disposal and agriculture (Kostandinou et al., 2009).

Emission inventories represent the amount of pollutants emitted to the atmosphere from a specific area (local to global) during a specific time period (past to future), originated from anthropogenic or natural activities (EPA, 2003; [http://en.wikipedia.org/wiki/Emission\\_inventory](http://en.wikipedia.org/wiki/Emission_inventory)).

Istanbul is one of the largest cities in the world with more than 12 million population and over 1.5 million cars according to 2008 Address Based Population Registration System, Turkish Statistical Institute, (TUIK, 2008). Rapid growths in urbanization and industrialization have occurred within the last 40 years. Through the emissions from the transport sector, a big portion of ozone precursors are emitted to the atmosphere. Liquefied petroleum gas (LPG) has been widely used by taxis from the beginning of 1998. Traffic rush hours clearly behave as a sink for ozone by the emissions of  $\text{NO}_x$ . There has also been a shift from coal to natural gas for domestic heating purposes starting from early 90's, leading to a decrease in the primary pollutant concentrations such as  $\text{SO}_x$  but an increase in secondary pollutant concentrations such as aerosols and ozone. The region experiences very dense industrial activities, almost the highest in the country. Based on Istanbul Chamber of Industry reports, 37% of the industrial activities in Istanbul comprise textile industry, 30% metal industry, 21% chemical industry, 5% food industry and 7% other industries. Low quality liquid fuels with high sulfur content, natural gas and LPG are the most commonly used fuel types in the industrial activities. Under all these dense and variety of industrial activities, Istanbul experiences very complex air quality conditions (Im et al., 2006 and 2008).



Air pollution becomes one of the important problems of the city together with traffic congestion as a result of increase population and unplanned urbanization. Based on reports of the State Statistical Institute published in 2006, one in five citizen in Istanbul owns a vehicle. The relationship between population and number of vehicles is illustrated in Figure 3.11. Both population and number of vehicles have an increasing trend after 1980s (Sertel et al., 2008).

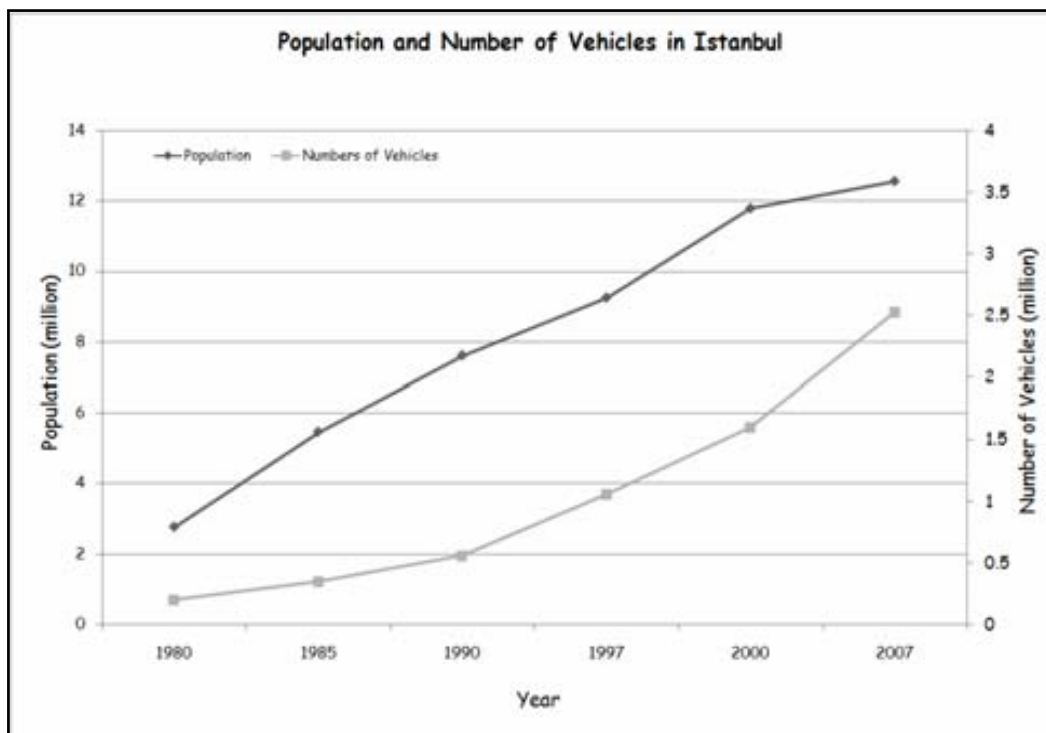


**Figure 3.11.** Population and Number of Vehicles in Istanbul (Sertel et al., 2008)

Emissions caused by the road traffic in Istanbul increased rapidly between years of 1990 and 2000, where the increase in CO, SO<sub>2</sub> and particulates were 50.1%, 55.7% and 82.5%, respectively (Becin, 2002). Road traffic is the dominant source category for most of the conventional pollutants such as CO, NO<sub>x</sub> and PM species. Road transport, alone, is responsible for 79 per cent of CO emissions and almost half of NO<sub>x</sub> emission totals (78 kt yr<sup>-1</sup>) (Kostandinos et al., 2009).

An important portion of NMVOCs also originate from road transport, although the major contributor to NMVOC emissions is found out to be solvent use. Solvent use contributes with 60 per cent of the total NMVOC emissions with the majority originating from commercial use. The largest share of SO<sub>x</sub> emissions stem from the industrial sector (96 kt yr<sup>-1</sup>). Industrial combustion emissions account for 54 per cent of the total SO<sub>x</sub> with the majority to originate from the combustion of coal (56 kt yr<sup>-1</sup>). The results of the study “Compilation of a High Spatially And Temporally Resolved emission Inventory For The Istanbul Greater Area Using GIS Technology (Kostandinos et al, 2009)” suggest that the two important air quality issues, PM and ozone pollution may highly be influenced locally from the road transport emissions. Thus, air pollution reduction strategies should be developed and implemented considering the sectoral distributions of emissions (Kostandinos et al., in preparation).

### **3.2.2. Observation**

Air pollution can cause health problems and it can also damage the environment and property. Measurement of air pollutants is important for preventive works in all over the world. Sulphur dioxide (SO<sub>2</sub>), particulate matter (PM), nitrogen oxides (NO<sub>x</sub>), carbon monoxide (CO) and hydrocarbons (HC) spread to Istanbul’s air from the pollution sources and they threaten human health (<http://www.yildiz.edu.tr/~kanat/Hava.html>).

Previously, measurements in Istanbul were inadequate and irregular. Since 1998, measurements have been done by Istanbul Metropolitan Municipality Environmental Protection Department with 8 immobile and 2 mobile vehicles. Five of them are on the European Side and three of them are on the Anatolian Side. There is one mobile station each side. Distribution of air quality measurement stations in Istanbul is shown in Figure 3.12. Stations are mainly positioned along the Bosphorus (EIES, 2005).

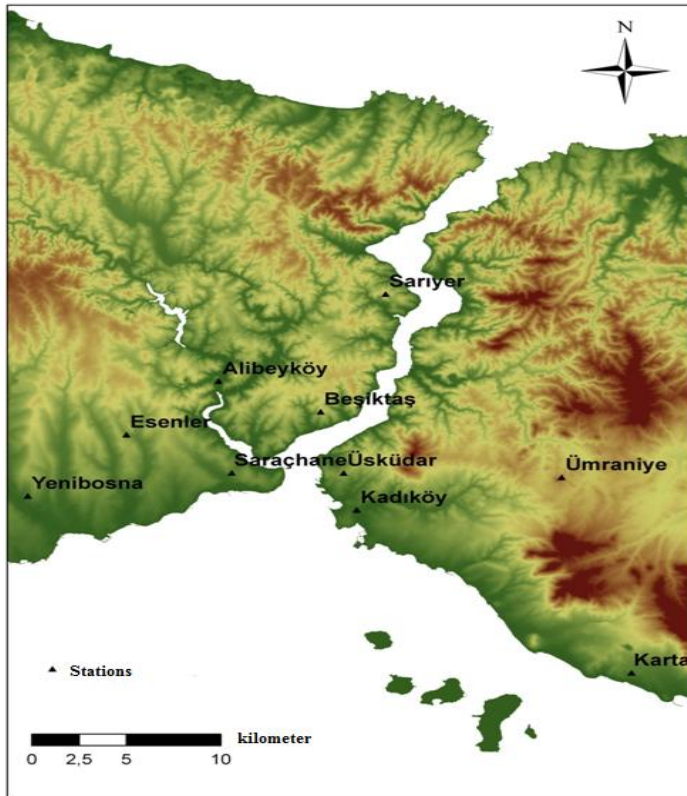


**Figure 3.12.** Distribution of Air Quality Measurement Stations in Istanbul (EIES, 2005)

In air quality measurement stations, data are stored daily, monthly and annually. The parameters measured at each station are shown in Table 3.2.

The air quality measurements initially have been made by the Institute of Sanitation at 17 stations between 1994 and 2000 and which decreased to ten between 2000 and 2007 (Sertel et al., 2008). Today's stations measure  $\text{CO}_2$ , CO,  $\text{NO}_x$ ,  $\text{SO}_2$ , particulates, VOC and NMVOC parameters and several others on daily basis for 365 days (EIES, 2005).

It is obvious that 10 stations are not enough to be able to display all the city's air profile. In addition, quality of the data is also a concern. As it is shown below, only 3 parameters ( $\text{SO}_2$ , PM and CO) are measured at all stations.

**Table 3.2.** Parameters Measured in Each Station (Istanbul Climate and Air Pollution Report, EIES, 2005)

<b>STATIONS</b>	<b>AIR POLLUTANTS</b>					
	<b><u>SO<sub>2</sub></u></b>	<b><u>NO<sub>x</sub></u></b>	<b><u>CO</u></b>	<b><u>O<sub>3</sub></u></b>	<b><u>HC</u></b>	<b><u>PM</u></b>
Yenibosna	X		X			X
Esenler	X	X	X		X	X
Saraçhane	X	X	X	X	X	X
Alibeyköy	X	X	X		X	X
Beşiktaş	X	X	X		X	X
Sarıyer	X		X			X
Üsküdar	X		X			X
Kadıköy	X	X	X	X	X	X
Ümraniye	X	X	X		X	X
Kartal	X		X			X

## 4. DATA AND METHODOLOGY

### 4.1. Data

Trajectory analysis is generally performed to evaluate air pollution transport patterns. In this study, this approach was used to evaluate the effects of Istanbul's air quality to other urban centers around Istanbul. A period of 30-year (1961-1990) NCEP/NCAR (National Centers for Environmental Predictions/National Centers for Atmospheric Research) reanalysis data (NNRP-NCEP NCAR Reanalysis Project -2.5°, 6-hourly) was used for a comprehensive climatological trajectory evaluation (Kindap et al., 2008).

The NCEP/NCAR Reanalysis 1 project is a state-of-the-art analysis/forecast system to perform data assimilation using past data from 1948 to the present in support of the needs of the research and climate monitoring communities. Input data is provided by compiling both observations from meteorological stations and model outputs. A large subset of this data is available from NCEP/NCAR in its original 4 times daily (at 0Z, 6Z, 12Z, and 18Z) format and as daily averages. Spatial coverage of data is the global grids of 2.5 degree x 2.5 degree (144 km x 73 km) 0.0E to 357.5E, 90.0N to 90.0S. There are 17 Pressure levels (1000, 925, 850, 700, 600, 500, 400, 300, 250, 200, 150, 100, 70, 50, 30, 20, 10) and 28 sigma levels (.995, .982, .964, .943, .916, .884, .846, .801, .751, .694, .633, .568, .502, .436, .372, .312, 258, .210, .168, .133, .103, .078, .058, .042, .029, .018, .010, .003) in the data. In this study, the distribution of trajectories was shown at  $\sigma = 0.950$  level (around 500 m), because topography does not affect air current at this level so, pollutants can distribute easily. Data obtained is updated daily in: pressure level, surface, surface fluxes, other fluxes, tropopause, derived data, spectral coefficients (<http://www.cdc.noaa.gov/cdc/data.ncep.reanalysis.html>).

Trajectories were computed according to the method described by Pettersen (1956) as a forward trajectory approach in an 81-km grid resolution (Pettersen, 1956).

An air parcel was released once every 6 hours for a total of 42,368 trajectories (air parcels) being released during the 30 years' period.

#### **4.2. Climatological Trajectory Approach**

The trajectory or path of a parcel is the curve described by the successive positions of the parcel. That is important to better understand the behaviour and potential impact of air pollution. The meteorological dynamics that cause air to rise or fall, and that determine its path can affect air quality by carrying air pollutants many miles from their sources. There are two types of trajectories: Forward and backward. Forward trajectories are drawn from the point of selected source to where the air parcel might arrive. Back trajectories show the pathway of air parcel from the end point to the possible source it might come from (Pettersen, 1956).

Fundamentally, the equations of motion, the equation of continuity, and such other equations as are required to constitute a complete set, state the relation between the time and the positions of individual parcels of air, but solutions applicable to the trajectory problem are not directly obtainable. Approximate trajectories can, however, be obtained from successive wind observations, using a method of successive approximations. To illustrate this method, for the time being, it is assumed that the motion is strictly horizontal (Pettersen, 1956).

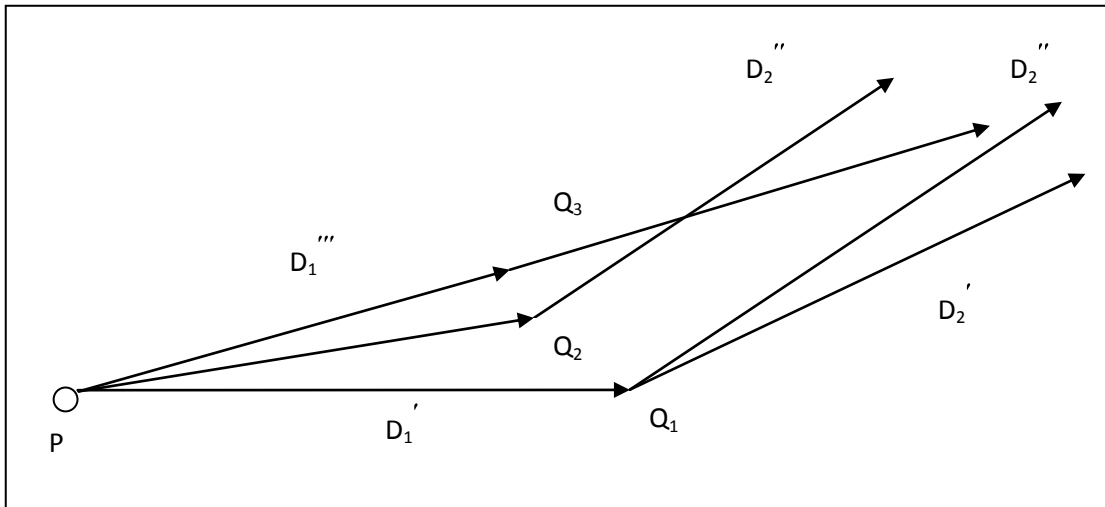


**Figure 4.1.** The Construction of Trajectories by Successive Approximations (Pettersen, 1956)

A series of wind charts at regular time intervals (1,2,3, etc.) are considered. Let  $P$  be the position on chart 1 occupied by the parcel whose trajectory is to be computed, and let  $V_1$  be the velocity vector. If there was no acceleration, the parcel at  $P$  would move a distance in the time interval  $(\Delta t)$  from chart 1 to chart 2, and arrive at the point  $Q_1$ , as shown in Figure 4.1.

$$D_1' = V_1 \Delta t \quad (4.2-1)$$

$V_1$ : initial velocity value,

$D_1'$ : distance for  $V_1$  and  $\Delta t$  time interval.

In the meantime, the velocity may have changed, and  $D_1'$  represents only a first approximation. To obtain a better approximation, we use the velocity  $V_2$  at  $Q_1$  on chart 2 to obtain the displacement  $D_2'$  from chart 1 to chart 2 that would have resulted if the parcel moved with a constant velocity  $V_2$ . The vectors  $D_1'$  and  $D_2'$  carry equal weights, and a second approximation is obtained by the mean of two displacements,

$$D_1'' = \frac{1}{2} (D_1' + D_2') \quad (4.2-2)$$

$D_1'$  : distance for  $V_1$  and  $\Delta t$  time interval,

$D_2'$  : distance for  $V_2$  and  $\Delta t$  time interval,

$D_1''$  : average of  $D_1' + D_2'$  .

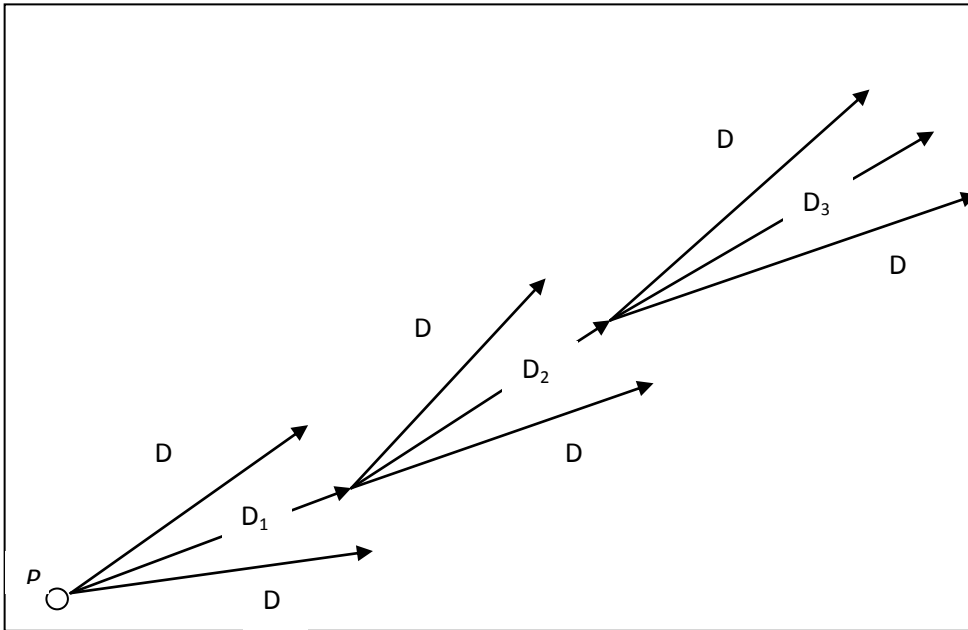


**Figure 4.2.** Second approximation is obtained by the mean of the two displacement (Pettersen, 1956).

This displacement takes the parcel to the point  $Q_2$  on chart 2. Next, we may use chart 2 and find the displacement  $D_2''$  of point  $Q_2$ , which may differ slightly from the displacement  $D_2'$ . A further approximation to the displacement would then be



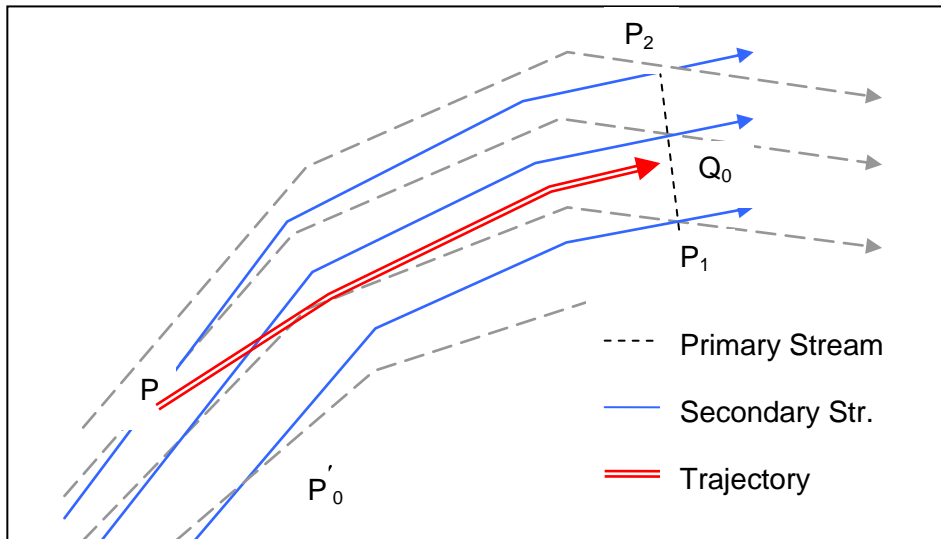


**Figure 4.3.** The construction of Trajectories From Streamlines and Isotach Charts (Pettersen, 1956)

$$D_1''' = \frac{1}{2} (D_1' + D_2'') \quad (4.2-3)$$

where  $D_1'''$  : average of  $D_1' + D_2''$ .

The operation may be repeated and, in general, it will be found that the points  $Q_1, Q_2, Q_3$ , etc., converge toward a point  $Q$ , which represents the position of the parcel at the end of the time interval  $\Delta t$ .

The procedure outlined above may be repeated from chart 2 to chart 3, etc. As shown in Figure 4.1., and a smooth curve through the points thus determined would represent the approximate trajectory (Pettersen, 1956)

If streamline and isotach charts are available, the trajectories are obtained most readily by the following procedure:

Let  $P_0$  in Fig. 4.2. be the point at the beginning of the computation, and let the wind speed at this point be  $V_0$ . If neither the streamline nor the wind speed changed, the parcel would travel a distance  $P_0 P_1 = V_0 \Delta t$  along the streamline through  $P_0$ .

1. Use the wind speed  $V_I$  at  $P_I$  and compute the distance  $P_I P_0 = V_0 \Delta t$  which the parcel would have traveled if the wind speed  $V_I$  and the second set of streamlines had remained unchanged.
2. Transfer the vector  $P_0'P_I$  to the position  $P_0 P_2$  (see the Fig. 4.3). A second approximation to the position of the parcel at the end of the interval would then be at  $Q_0$ .
3. Draw the smooth curve  $P_0Q_0$  such that it is tangent to the first set of streamlines at  $P_0$  and to the second set of streamlines at  $Q_0$ .
4. Measure the distance  $P_0Q_0$  and compare it with the distance  $D = V \Delta t$ , where  $V$  is the mean wind speed (obtained from the two sets of isotach charts) along the approximate trajectory  $P_0Q_0$ . If the two distances do not agree, the end point must be adjusted.

In this study, during 30 years, the probability of the arrival of the trajectories (T) to a given grid cell (ij) is equal to the number of trajectories crossing this grid cell ( $N_{ij}$ ) divided by the number of air trajectories released ( $N_{tot}$ ).

$$T_{ij} = N_{ij} / N_{tot} \quad (4.2-4)$$

The computed probability is dependent on the grid size and the trajectory length. In general, the probability of the arrival increases with the length of the trajectories, but for trajectories longer than 8 days it does not change much (Saltbones et al., 2000). In this study, 10-day trajectories were considered (Kindap et al., 2008).

### 4.3. MM5 Mesoscale Meteorological Model

The PSU/NCAR mesoscale model is a limited-area, nonhydrostatic terrain-following sigma-coordinate model designed to simulate or predict mesoscale and regional-scale atmospheric circulation. It has been developed at Penn State and NCAR as a community mesoscale model and is continuously being improved by contributions from users at several universities and government laboratories (Grell et al., 1994; [http://www.mmm.ucar.edu/mm5/documents/MM5\\_tut\\_Web\\_notes/tutorialTOC.htm](http://www.mmm.ucar.edu/mm5/documents/MM5_tut_Web_notes/tutorialTOC.htm)).

The Fifth-Generation NCAR / Penn State Mesoscale Model (MM5) is the latest in a series that developed from a mesoscale model used by Anthes at Penn State in the early 70's that was later documented by Anthes and Warner (1978). Since that time, it has undergone many changes designed to broaden its usage. This include (i) a multiple-nest capability, (ii) nonhydrostatic dynamics, which allows the model to be used at a few-kilometer scale, (iii) multitasking capability on shared- and distributed-memory machines, (iv) a four-dimensional data-assimilation capability, and (v) more physics options (Anthes et al., 1978).

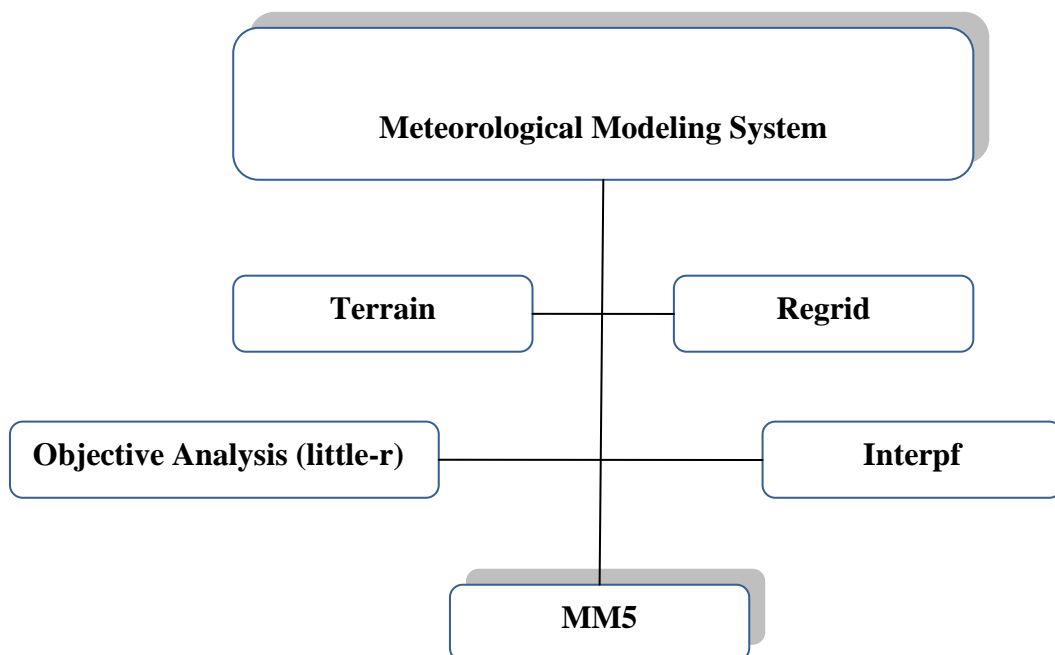


**Figure 4.4.** The MM5 Modeling System Flow Chart (Kindap, 2005)

### 4.3.1. The MM5 Model Horizontal and Vertical Grid

It is useful to first introduce the model's grid configuration. The modeling system usually gets and analyzes its data on pressure surfaces, but these have to be interpolated to the model's vertical coordinate before being input to the model. The vertical coordinate is terrain following meaning that the lower grid levels follow the terrain while the upper surface is flat. Intermediate levels progressively flatten as the pressure decreases toward the chosen top pressure. A dimensionless quantity  $\sigma$  is used to define the model levels

$$\sigma = (p - p_t) / (p_s - p_t) \quad (4.3.1-1)$$

where  $p$ : reference-state pressure,

$p_t$ : a specified constant top pressure, and  $p_s$  : the reference-state surface pressure

At the model top  $\sigma$  is zero and at the model surface it is one, and each model level is defined by a value of  $\sigma$ . The model vertical resolution is defined by a list of values between zero and one that do not necessarily have to be evenly spaced. Commonly the resolution in the boundary layer is much finer than above, and the number of levels may vary from ten to forty, although there is no limit in principle ([http://www.mmm.ucar.edu/mm5/documents/MM5\\_tut\\_Web\\_notes/tutorialTOC.htm](http://www.mmm.ucar.edu/mm5/documents/MM5_tut_Web_notes/tutorialTOC.htm)).

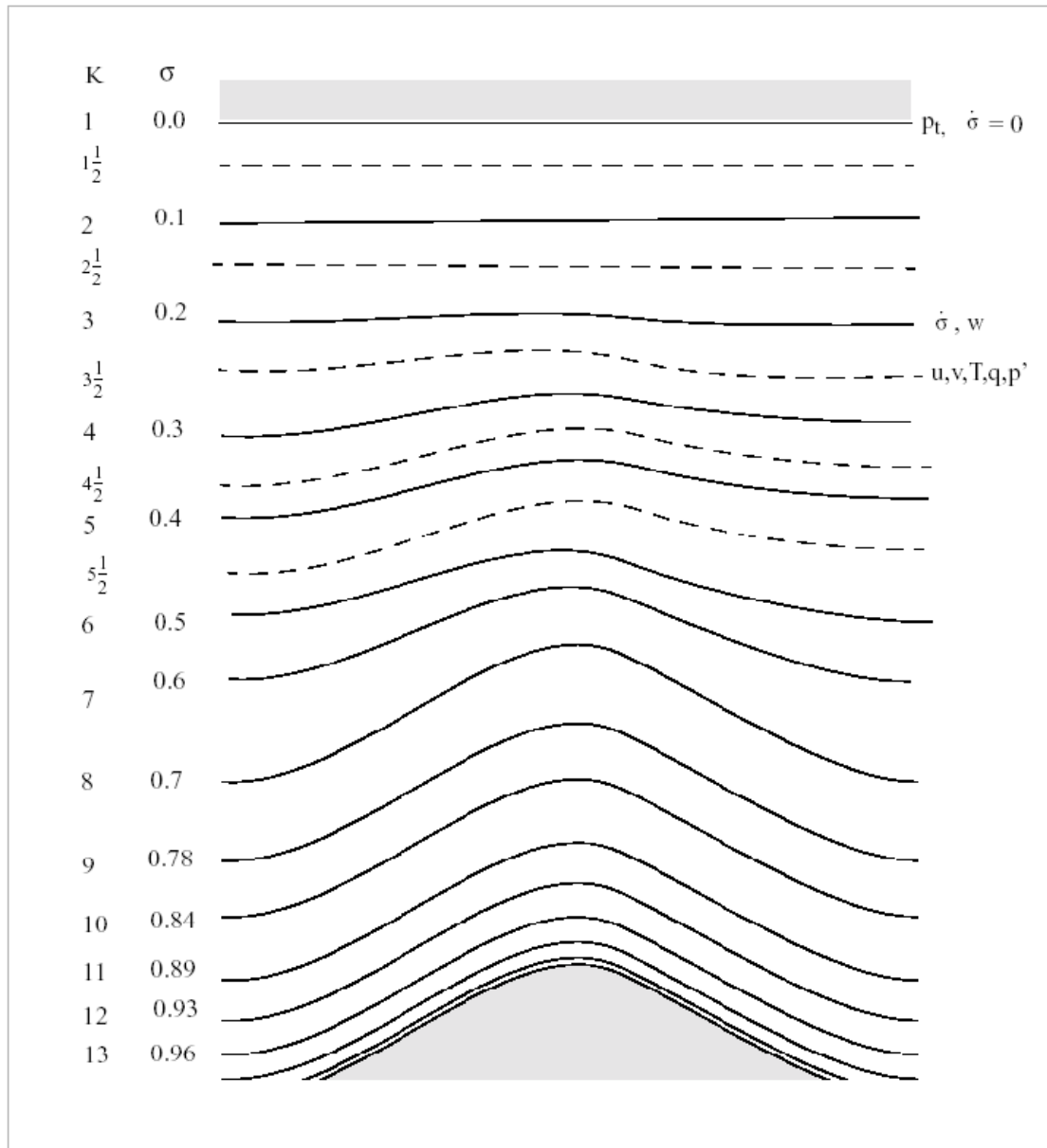


**Figure 4.5.** Schematic Representation of the Vertical Structure of the Model

([http://www.mmm.ucar.edu/mm5/documents/MM5\\_tut\\_Web\\_notes/tutorialTOC.htm](http://www.mmm.ucar.edu/mm5/documents/MM5_tut_Web_notes/tutorialTOC.htm))

The horizontal grid has an Arakawa-Lamb B-staggering of the velocity variables with respect to the scalars. This is shown in Fig 4.6. where it can be seen that the scalars (T, q etc.) are defined at the center of the grid square, while the eastward (u) and northward (v) velocity components are collocated at the corners. The center points of the grid squares will be referred to as cross points, and the corner points are dot points. Hence horizontal velocity is defined at dot points, for example, and when data is input to the model the

preprocessors do the necessary interpolations to assure consistency with the grid ([http://www.mmm.ucar.edu/mm5/documents/MM5\\_tut\\_Web\\_notes/tutorialTOC.htm](http://www.mmm.ucar.edu/mm5/documents/MM5_tut_Web_notes/tutorialTOC.htm)).

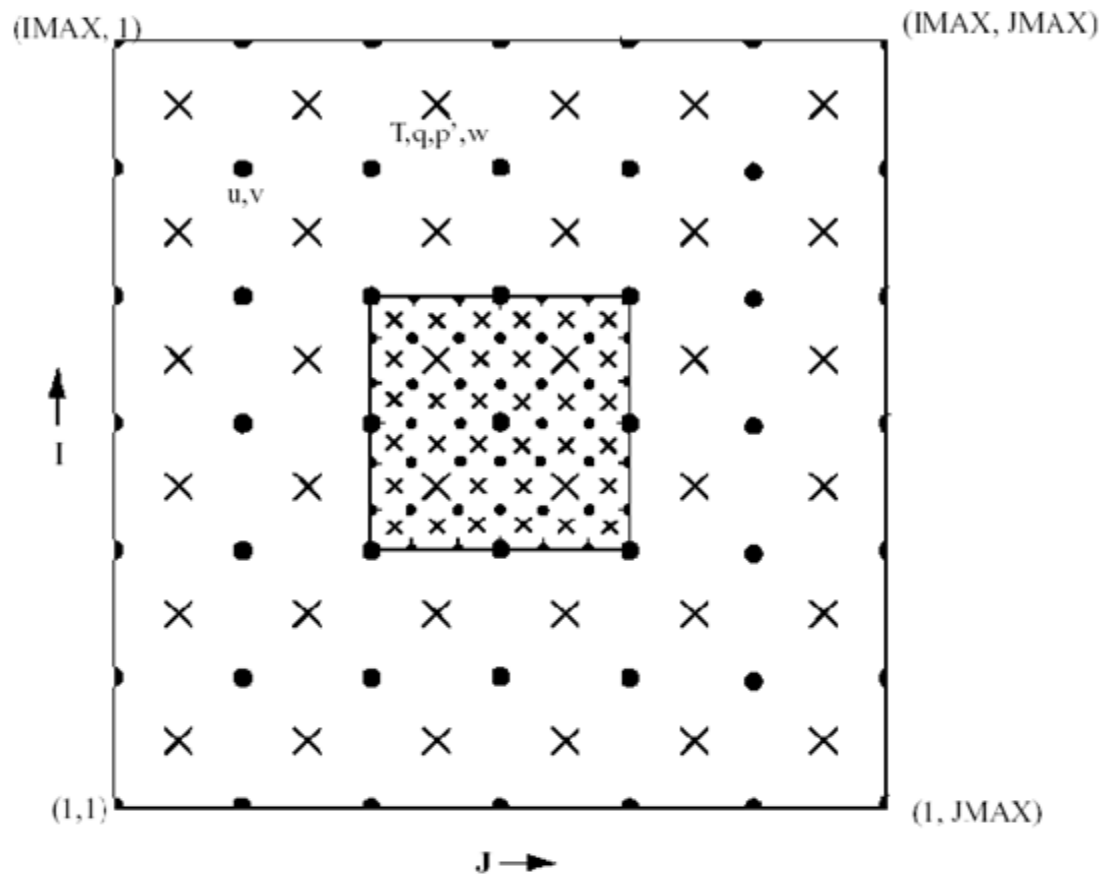


**Figure 4.6.** Schematic Representation Showing the Horizontal Arakawa B-grid Staggering of the Dot (I) and Cross (x) Grid Points

([http://www.mmm.ucar.edu/mm5/documents/MM5\\_tut\\_Web\\_notes/tutorialTOC.htm](http://www.mmm.ucar.edu/mm5/documents/MM5_tut_Web_notes/tutorialTOC.htm))

The best way to understand how the MM5 model operates is to explain the main routines it uses to accomplish a numerical simulation. The TERRAIN program horizontally interpolates the regular latitude-longitude elevation and vegetation onto the chosen mesoscale domain; it then outputs data files that are used by the REGRID. The REGRID program reads meteorological analyses on pressure levels and interpolates them from some native grid and map projection to the grid and map projection defined by TERRAIN; it then creates data files useable by INTERPF. The INTERPF routine handles data transformations that are necessary to put analysis data into a format useable by the

mesoscale model. INTERPF ingests data from REGRID, performs vertical interpolation, diagnostic computation, and data reformatting to create initial, lateral boundary, and lower boundary conditions for the mesoscale model. The MM5 program is the numerical weather prediction portion of the modeling system (Kindap, 2005).

#### **4.3.2. Terrain**

TERRAIN, makes use of high-resolution global terrain and land use data sets to create static files for the domain. The static files currently include values for each grid point for terrain height and land use specification (e.g., deciduous forest, desert, water). This is essential for an accurate run. It also defines the model domain and map projection that locates the area the model will simulate. Various types of terrain affect atmospheric circulation patterns. Therefore, the type of terrain and vegetation cover must be specified and accurately defined within the chosen domain for the simulation to produce accurate results (Guo and Chen, 1994).

The purpose of TERRAIN is to create the terrain height and land-use on the mesoscale model grids from the regular latitude-longitude interval source terrain height and land-use characteristics data.

TERRAIN horizontally interpolates (or analyzes) the regular latitude - longitude terrain elevation, and vegetation (land use) onto the chosen mesoscale domains. If the land-surface model (LSM) will be used in the MM5 model, additional fields such as soil types, vegetation fraction, and annual deep soil temperature will also be generated. The data available as input to the program TERRAIN include terrain elevation, landuse/vegetation, land-water mask, soil types, vegetation fraction and deep soil temperature. Most data are available at six resolutions: 1 degree, 30, 10, 5 and 2 minutes, and 30 seconds ([http://www.mmm.ucar.edu/mm5/documents/MM5\\_tut\\_Web\\_notes/tutorialTOC.htm](http://www.mmm.ucar.edu/mm5/documents/MM5_tut_Web_notes/tutorialTOC.htm)).

The model has the option of three sets of land-use categorizations ( that are assigned along with elevation in the TERRAIN program from archived data. These have 13, 16, or 24 categories (type of vegetation, desert, urban, water, ice, etc.). Each grid cell of the

model is assigned one of the categories, and this determines surface properties such as albedo, roughness length, longwave emissivity, heat capacity and moisture availability. Additionally, if a snow cover dataset is available, the surface properties may be modified accordingly. The values in the table are also variable according to summer or winter season (for the northern hemisphere), (Kindap, 2005), ([http://www.mmm.ucar.edu/mm5/documents/MM5\\_tut\\_Web\\_notes/tutorialTOC.htm](http://www.mmm.ucar.edu/mm5/documents/MM5_tut_Web_notes/tutorialTOC.htm)).

A simpler land-use option distinguishes only between land and water, and gives the user control over the values of surface properties for these categories.

In this study, gridded hourly emissions data which were obtained from the TERRAIN module of MM5 have been used for biogenic sources. This database provides emissions for biogenic source sector. As a result, land use data is the most important part of the calculation of biogenic emissions. In this study, a 24-category, global coverage with the resolution of 5 minutes, USGS landuse/vegetation data has been used (Table 4.1.). This dataset includes 24 different categories for land-use and is based upon U.S. Geological Survey (USGS) criteria (Kindap, 2005). Emission factors as well as correction factors for estimating total emissions are based upon previous publications (Simpson et al., 1999).



**Table 4.1.** Description of 24-Category (USGS) Land-Use Categories (Kindap, 2005)

<b>Vegetation Identification</b>	<b>Vegetation Description</b>	<b>Vegetation Identification</b>	<b>Vegetation Description</b>
1	Urban	13	Evergrn. Broadlf.
2	DryInd Crop. Past.	14	Evergrn. Needlf.
3	Irrg. Crop. Past.	15	Mixed Forest
4	Mix. Dry/Irrg. C.P.	16	Water Bodies
5	Crop./Grs. Mosaic	17	Herb. Wetland
6	Crop./Wood Mosc	18	Wooded Wetland
7	Grossland	19	Bar. Sparse Veg.
8	Shrubland	20	Herb. Tundra
9	Mix Shrb./Grs.	21	Wooden Tundra
10	Savanna	22	Mixed Tundra
11	Decids. Broadlf.	23	Bare Grnd. Tundra
12	Decids. Needlf.	24	Snow or Ice

### 4.3.3. Regrid

The purpose of REGRID is to read archived gridded meteorological analyses and forecasts on pressure levels and interpolate those analyses from some native grid and map projection to the horizontal grid and map projection as defined by the MM5 preprocessor program TERRAIN. The input analyses were obtained from the NCEP (The National Centers for Environmental Prediction) database. This data set is a global analysis beginning in 1948 using a single analysis system for the entire dataset. Analyses are available every six hours. Data are archived on a 2.5 x 2.5 degree lat/lon grid and a gaussian grid (~1.9 degrees lat, 2.5 degrees lon) (Kindap, 2005).

After the simulation domain had been established, the program REGRID was run to process the meteorological background fields. REGRID generated first-guess fields for the model simulation by horizontally interpolating a larger-scale data set (global or regional coverage) to the simulation domain. REGRID interpolated the background fields to the simulation domain throughout the simulation period; these files were used ultimately to generate lateral boundary conditions for the coarse-domain simulations ([http://www.mmm.ucar.edu/mm5/documents/MM5\\_tut\\_Web\\_notes/tutorialTOC.htm](http://www.mmm.ucar.edu/mm5/documents/MM5_tut_Web_notes/tutorialTOC.htm)).

### 4.3.4. Interpf

The INTERPF program sets the initial and boundary conditions for the meteorology simulation. In the program, the analyses from one time were interpolated to provide MM5's initial conditions, while analyses from all running times were interpolated to get MM5's lateral boundary conditions. This was the final step before the actual MM5 model could be run (Kindap, 2005).

#### 4.3.5. MM5

This is the numerical weather prediction part of the modeling system. MM5 can be used for a broad spectrum of theoretical and real-time studies, including applications of both predictive simulation and four-dimensional data assimilation to monsoons, hurricanes, and cyclones. On the smaller meso-beta and meso-gamma scales (2-200 km), MM5 can be used for studies involving mesoscale convective systems, fronts, land-sea breezes, mountain-valley circulations, and urban heat islands (Kindap, 2005).

MM5 is based on primitive physical equations of momentum, thermodynamics, and moisture. The state variables are temperature, specific humidity, grid-relative wind components, and pressure. MM5 model has physical options for radiation, convective parameterization, PBL (Planetary Boundary Layer) processes, surface layer processes ([http://www.mmm.ucar.edu/mm5/documents/MM5\\_tut\\_Web\\_notes/tutorialTOC.htm](http://www.mmm.ucar.edu/mm5/documents/MM5_tut_Web_notes/tutorialTOC.htm)).

## 5. RESULTS AND DISCUSSIONS

### 5.1. Results of the Climatological Trajectory Approach

The goal of this study is to present the impact of the air pollution in Istanbul to its surroundings, especially to the some neighboring towns.

A period of 30-year (1961-1990) NCEP/NCAR (National Centers for Environmental Predictions/National Centers for Atmospheric Research) reanalysis data (NNRP-NCEP NCAR Reanalysis Project -2.5°) was used for a comprehensive climatological trajectory evaluation. The distribution of trajectories was shown at  $\sigma = 0.950$  level. The trajectories were computed according to a method described by Pettersen (1956) as a forward trajectory approach in an 81-km grid resolution. An air parcel was released once every 6 hour and a total of 42,368 air parcels were released during these 30 years (1961-1990) (Kindap et al., 2008).

For 10-day period, as 4xdaily times (00Z, 06Z, 12Z and 18Z), almost total 40.000 trajectories were sent. For example; for 06Z of 1<sup>st</sup> day of 12<sup>th</sup> month, main air movement (as an average of 30 years) was described by evaluating data of each year at that specific time. The study was conducted like that for all period.

Evaluations were made for 4 seasonal periods (3-month duration), and on annual basis. Monthly simulations show similar distribution to its own seasonal one. In general, the probability of the arrival increases with the length of the trajectories, but for trajectories longer than 8 days it does not change much (Saltbones et al., 2000). In this study, therefore, 10-day trajectories were studied. Longer periods gave similar results with 10-day period.

For the selected cities, detailed information (number of arrival trajectories for each receptor, probability of arrival and average travel time) is listed in Table 5.1. Besides, the probability of trajectory distribution are presented in the previous figures for four seasonal

periods and annually. In addition, the average travel time was computed by calculating the number of points along the trajectories (every 6 hour) from Istanbul to its surroundings and it is shown in the latter figures for four seasonal periods and annually.

**Table 5.1.** Number of Arriving, Probability of Arrival, and Average Travel Time from Istanbul to Selected Cities (W:Winter, Sp:Spring, Su:Summer, A:Autumn, Y:Year)

Selected Receptors City Number and Name	Number of Arrival Trajectories for Each Receptor					Probability of Arrival For Each Receptor (%)					Average Travel Time For Each Receptor (h)				
	W	Sp	Su	A	Y	W	Sp	Su	A	Y	W	Sp	Su	A	Y
<b>0 - Athene</b>	695	743	318	696	2460	6.42	6.73	2.98	6.37	5.81	24-48	24-48	24-48	24-48	24-48
<b>1 - İzmir</b>	<b>1500</b>	<b>2099</b>	<b>2764</b>	<b>2205</b>	<b>8496</b>	<b>13.85</b>	<b>19.01</b>	<b>25.90</b>	<b>20.19</b>	<b>20.05</b>	<b>12-24</b>	<b>12-24</b>	<b>12-24</b>	<b>12-24</b>	<b>12-24</b>
<b>2 - Crete</b>	623	699	1000	1016	3337	5.75	6.33	9.37	9.30	7.88	24-48	24-48	24-48	24-48	24-48
<b>3 - Antalya</b>	<b>502</b>	<b>962</b>	<b>910</b>	<b>620</b>	<b>3064</b>	<b>4.64</b>	<b>8.71</b>	<b>8.53</b>	<b>5.68</b>	<b>7.23</b>	<b>24-48</b>	<b>24-48</b>	<b>24-48</b>	<b>24-48</b>	<b>24-48</b>
<b>4 - Sinop</b>	577	536	72	340	1524	5.33	4.86	0.67	3.11	3.60	24-48	24-48	24-48	24-48	24-48
<b>5 - Ankara</b>	<b>516</b>	<b>852</b>	<b>263</b>	<b>560</b>	<b>2259</b>	<b>4.77</b>	<b>7.72</b>	<b>2.46</b>	<b>5.13</b>	<b>5.33</b>	<b>24-48</b>	<b>24-48</b>	<b>24-48</b>	<b>24-48</b>	<b>24-48</b>
<b>6 - Cairo</b>	230	331	560	313	1453	2.12	3.00	5.25	2.87	3.43	72-96	72-96	72-96	72-96	72-96
<b>7 - Bucuresti</b>	<b>232</b>	<b>335</b>	<b>37</b>	<b>202</b>	<b>822</b>	<b>2.14</b>	<b>3.03</b>	<b>0.35</b>	<b>1.85</b>	<b>1.94</b>	<b>24-48</b>	<b>24-48</b>	<b>24-48</b>	<b>24-48</b>	<b>24-48</b>
<b>8 - Roma</b>	93	64	2	65	238	0.86	0.58	0.02	0.60	0.56	96-120	96-120	120-144	120-144	96-120
<b>9 - Sofia</b>	<b>333</b>	<b>377</b>	<b>50</b>	<b>268</b>	<b>1056</b>	<b>3.08</b>	<b>3.41</b>	<b>0.47</b>	<b>2.45</b>	<b>2.49</b>	<b>24-48</b>	<b>24-48</b>	<b>24-48</b>	<b>24-48</b>	<b>24-48</b>
<b>10 - Nicosia</b>	366	640	477	338	1899	3.38	5.80	4.47	3.10	4.48	24-48	24-48	24-48	24-48	24-48
<b>11 - Kiev</b>	<b>86</b>	<b>104</b>	<b>13</b>	<b>104</b>	<b>315</b>	<b>0.79</b>	<b>0.94</b>	<b>0.12</b>	<b>0.95</b>	<b>0.74</b>	<b>72-96</b>	<b>72-96</b>	<b>72-96</b>	<b>72-96</b>	<b>72-96</b>
<b>12 - Beirut</b>	282	349	310	240	1227	2.60	3.16	2.90	2.20	2.90	48-72	48-72	48-72	48-72	48-72

The number and probability of arrival trajectories and average travel time for each receptor city are presented in Table 5.1. Furthermore, graph of the number and probability of arrival trajectories are presented in Figure 5.2. According to the both Table 5.1. and Fig. 5.1; İzmir may be mostly affected by the distribution of air trajectories during a 12-24 hour period. On the other hand, although Bucuresti is nearly three times closer to Istanbul than Cairo, Cairo experiences higher probability of trajectory arrival than Bucuresti. As compared with the other selected cities, Rome has the least influence because of its location.

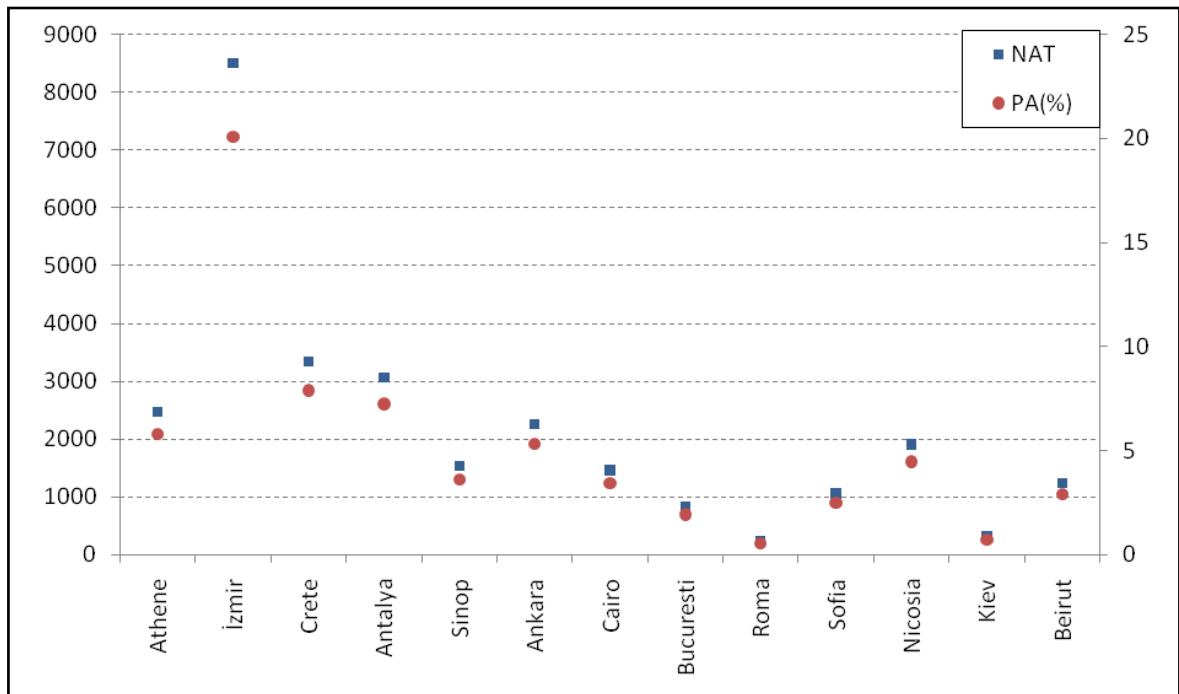


**Figure 5.1.** Graph of the Number of Arrival Trajectories and the Probability of Arrival (%)

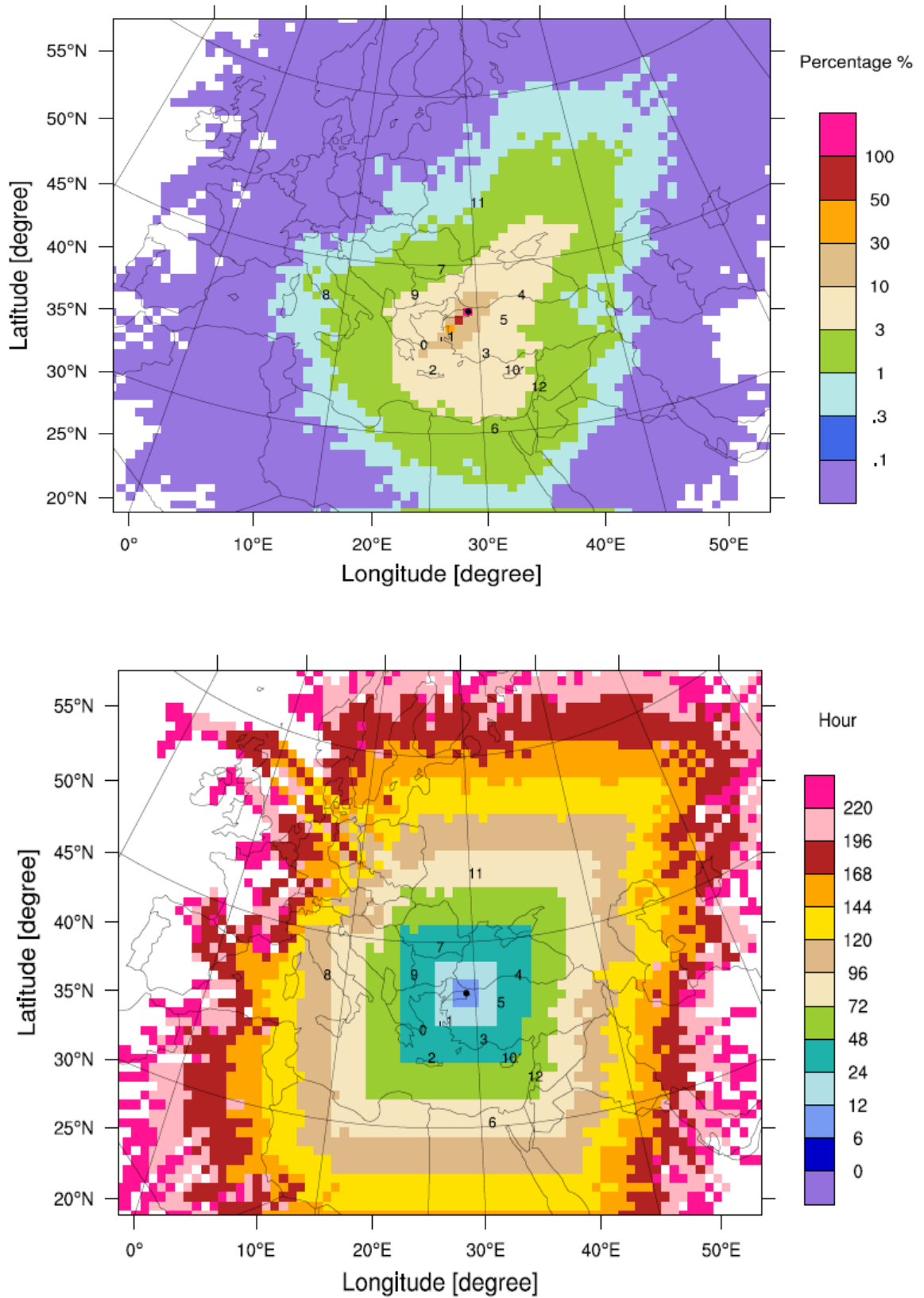


**Figure 5.2.** Maps of a) The Air Distribution and b) Average Travel Times From Istanbul to the Selected Cities for Winter Duration (12<sup>th</sup>, 1<sup>st</sup> and 2<sup>nd</sup> Months)



The direction of the distribution of air trajectories from Istanbul to its surroundings for the winter period is the Northeast-Southwest, shown in Figure 5.2.a. Besides, as it is shown in Fig. 3.6., North-East winds are the effective winds for the west part of Turkey in the winter period. As it can be seen in the figure, Bursa ( $\geq 50\%$ ) and Çanakkale (30-50%) are the most affected cities from Istanbul's air quality in winter months. In addition, it is shown that the south-west and the north-east region of Istanbul (in this region, Izmir and Athens have 10-30%) are affected secondarily. Other cities are exposed to less than 10 per cent of distribution. It can be said that, in the western part of Turkey, northeast wind (with the impact of high pressure region in East Europe) is effective in winter duration. On the other hand, Figure 5.2.b. shows the average travel time of air trajectories. Nine of the selected cities might be affected in a-two day-period.

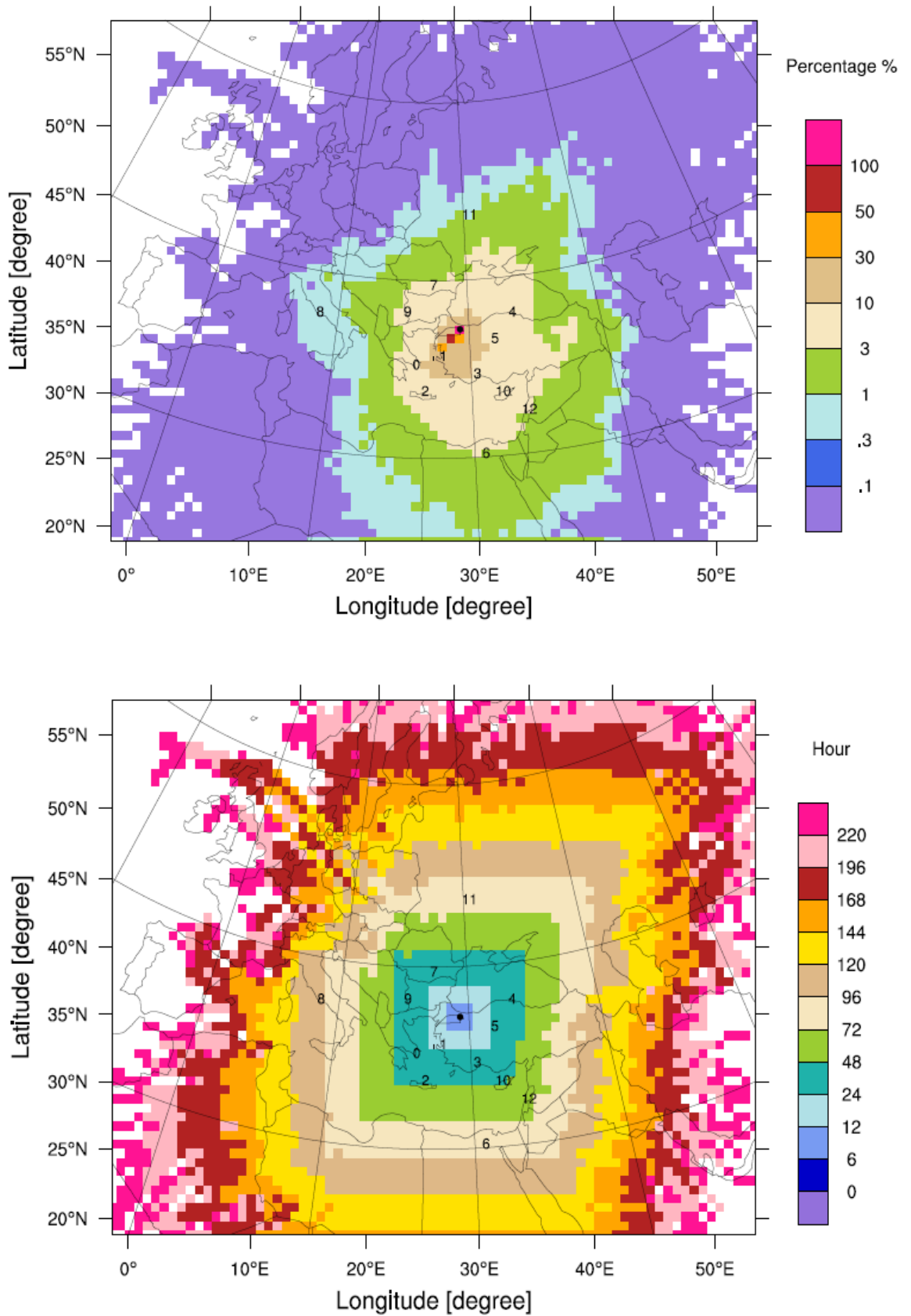


**Figure 5.3.** Maps of a) The Air Distribution and b) Average Travel Times From Istanbul to the Selected Cities for Winter Duration (12<sup>th</sup>, 1<sup>st</sup> and 2<sup>nd</sup> Months)

As seen in Fig. 5.3.a., the distribution is more circular than the distribution of winter. Because of this circular distribution, cities which are on the east (Ankara, Nicosia and Beirut) and the west (Sofia, Bucuresti and Athens) part of Istanbul, might be affected mostly in this period. Besides, main wind direction of this period, shown in Fig. 3.7., is North-East. On the other hand, Figure 5.3.b. presents the average travel time of air trajectories. It can be said that nine of the selected cities might be affected in a two-day period.

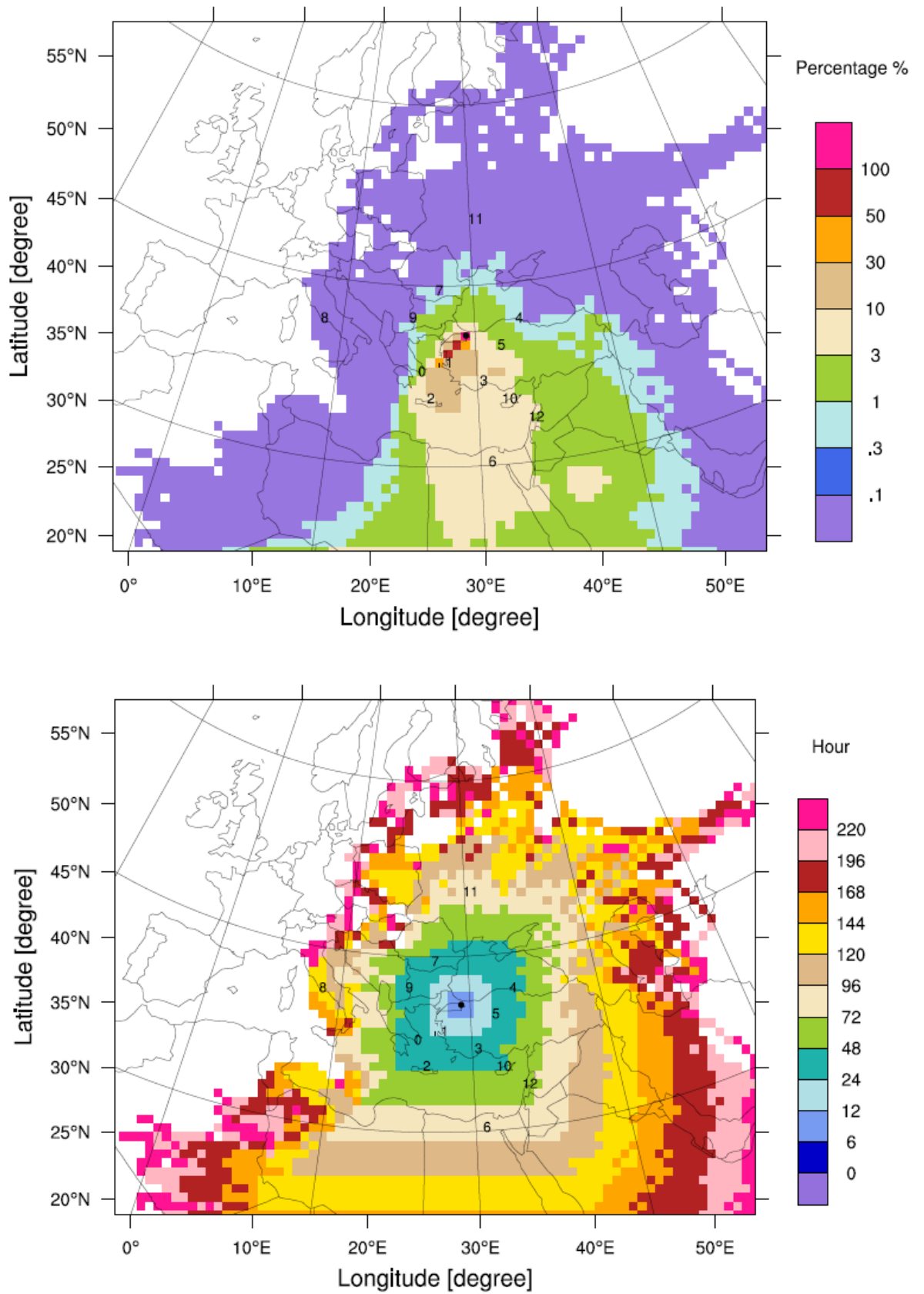


**Figure 5.4.** Maps of a) The Air Distribution and b) Average Travel Time From Istanbul to the Selected Cities for Summer Duration (6<sup>th</sup>, 7<sup>th</sup> and 8<sup>th</sup> months)

Evaluations show that main direction of air trajectory transport is the South and the South-West, see Figure 5.4.a. In addition, since Basra Low Pressure Center affects our country from the South and the South-East in summer, dominant wind direction of this period is from the North-Northeast (shown in Fig.3.8.) to the South with the impact of both Basra Low Pressure Center and Azor High Pressure Center (Komuscu, 2001).

The results also show that Athens is affected with a 6.42 % range in winter months and 3 % in summer months. On the other hand, Antalya, İzmir, Cairo and Girit are affected twice higher in summer than in winter. Sinop and Ankara are affected from Istanbul's air quality in winter months more than in summer months because of main northeast wind. Sofia and Kiev are affected mainly in the winter period. Figure 5.4.b. shows the average travel time of air trajectories. While average travel times of the cities are the same for all seasonal periods, only average travel times of Rome for summer and autumn periods (120-144 h) differ from the other periods (96-120 h).

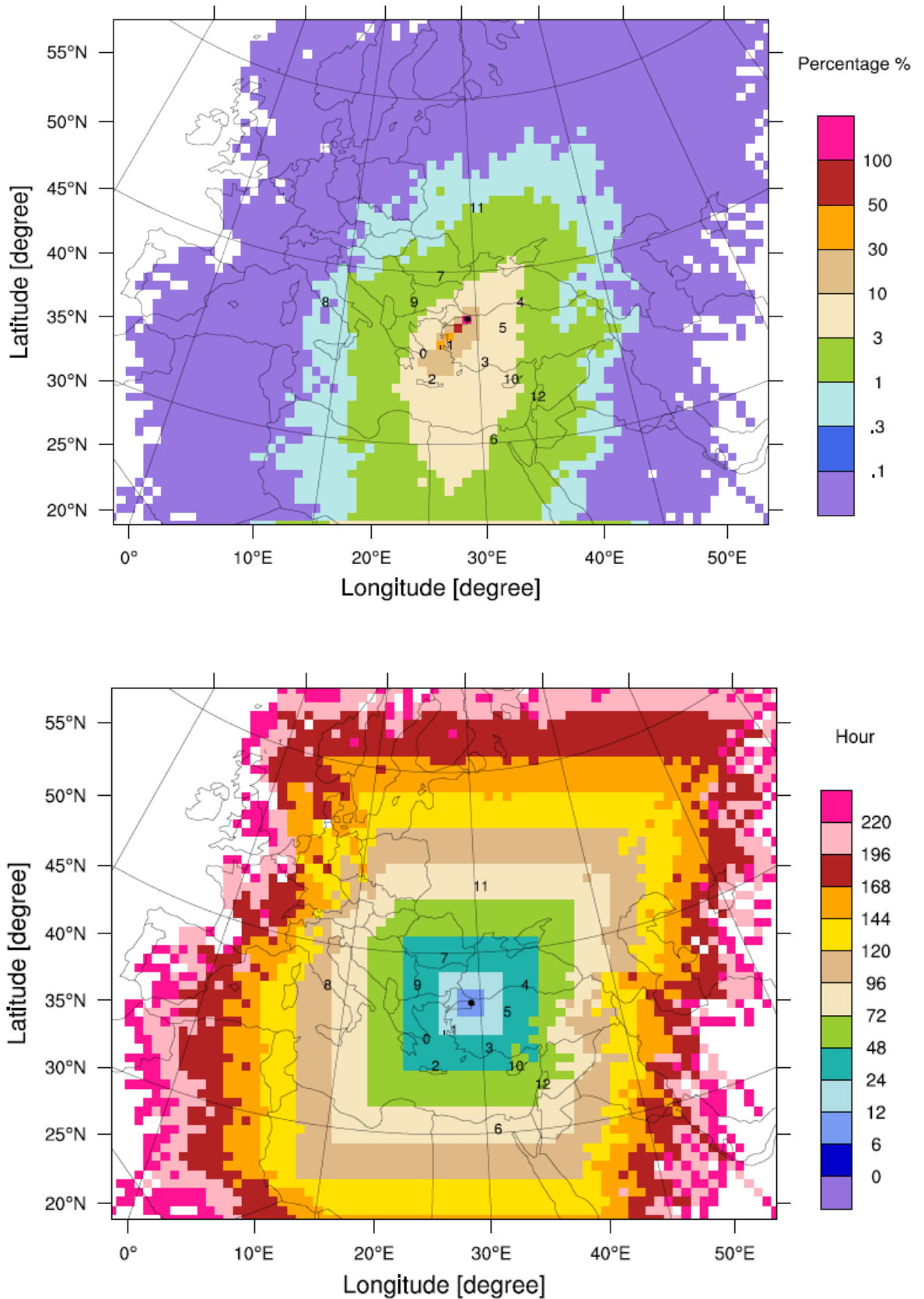


**Figure 5.5.** Maps of a) The Air Distribution and b) Average Travel Time From Istanbul to the Selected Cities for Autumn Duration (9<sup>th</sup>, 10<sup>th</sup> and 11<sup>th</sup> months)

Figure 5.5.a. presents the air distributions for autumn period. According to the result of the evaluation for the autumn period, the direction of air movement is mainly the Northeast-Southwest like winter months. Besides, main wind direction of this period is North-Northeast, in Fig. 3.9. On the other hand, Figure 5.5.b. presents the average travel time of air trajectories. It can be said that eight of the selected cities might be affected in a two day-period.

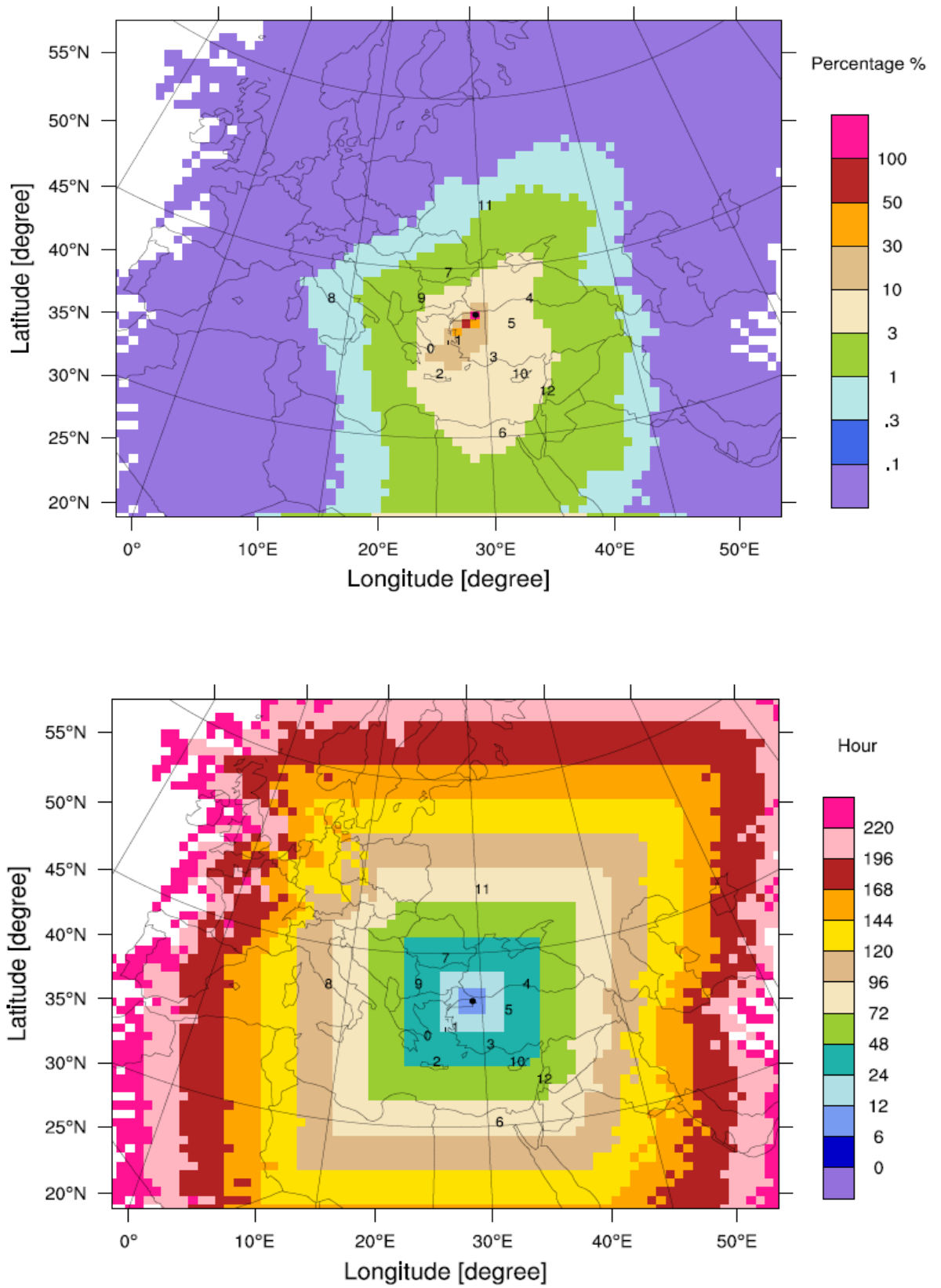


**Figure 5.6.** Maps of a) The Air Distribution and b) Average Travel Time From Istanbul to the Selected Cities for Annually



Evaluation for one-year period shows that the main direction of air distribution (Fig. 5.6.a.) and wind direction (Fig. 3.10.) in selected part is from the North and North-East to the South and South-East. The annual distribution is nearly same with the distributions for seasonal periods except the summer one. In the summer period, mostly the South and the South-West parts of Istanbul might be affected. On the other hand, the latter figure (Fig.5.6.b.) presents the average travel time of air trajectories. It can be said that nine of the selected cities might be affected in a-two day-period.

Air pollution in Istanbul mostly affects the cities in the South and South-East part (Bursa, Çanakkale and Izmir) of Istanbul. If it is thought that air pollution in Bursa is serious because of the industrial activities and urbanization, the air movement from Istanbul to Bursa brings extra pollution load.

In conclusion, generally air movement changes according to the wind direction. It can be said that air pollution in Istanbul may be distributed to large areas throughout the year.

### **5.1. A Case Study for a Specific Episode Using MM5**

In the first part of the study, air trajectories using NNRP for a 30-year period were presented. This section presents a case study for a selected episode (22- 25 July 2002, at 950 mb) using the MM5 model. The aim of selecting this period is that; different wind directions were seen on Istanbul and its surroundings. Trajectories were generated for 22, 23, 24 and 25 July 2002, beginning at 00:00, for a 24-hour period. Forward trajectories were sent from 6 different points in Istanbul. 27-km grids were prepared. Forward trajectories, wind directions and sea level pressures are shown in following figures.

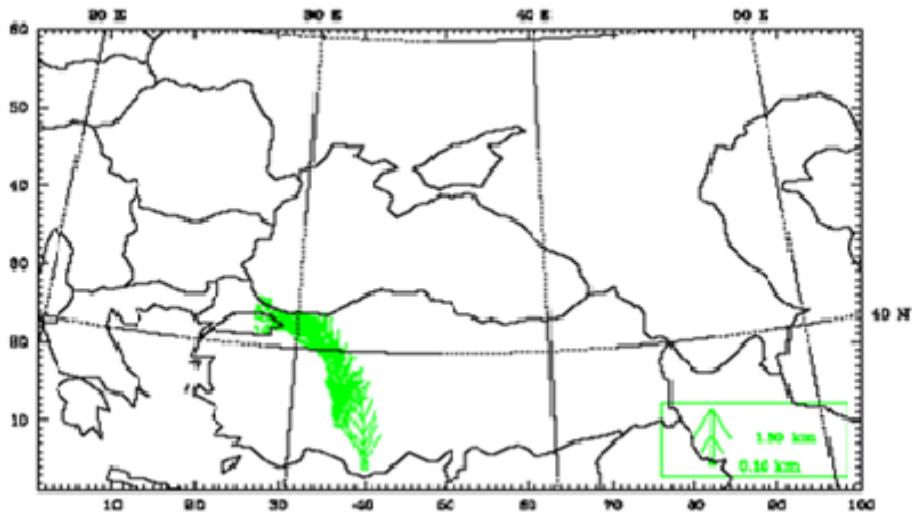


**Figure 5.7.** MM5 Forward Trajectory Approach for 22 July 2002

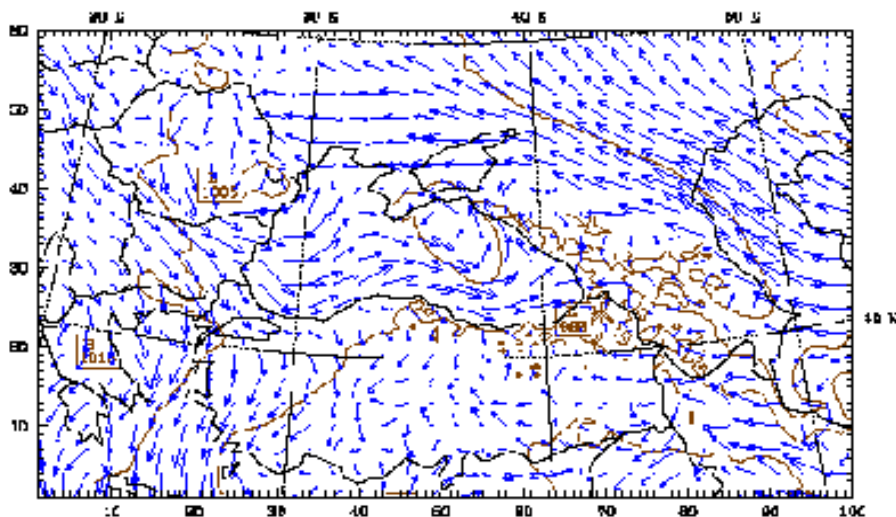


**Figure 5.8.** Wind Direction and Sea Level Pressure for 22 July 2002

On 22 July, 2002, the direction of air trajectories, shown in Figure 5.7., is South and South-East. After a 24-hour period, trajectories arrive the South border of Turkey. Trajectories can rise up to 1.60 km. Wind directions for that day is shown in Figure 5.8. According to the figure, North-Western winds come from the Balkans and affects the Marmara Region. There is a low pressure center on Black Sea. Different wind directions are seen on Turkey. It can be said that; Adapazarı, Bursa, Eskişehir, Ankara, Konya, Mersin were affected the air transport from Istanbul on 22 July 2002.

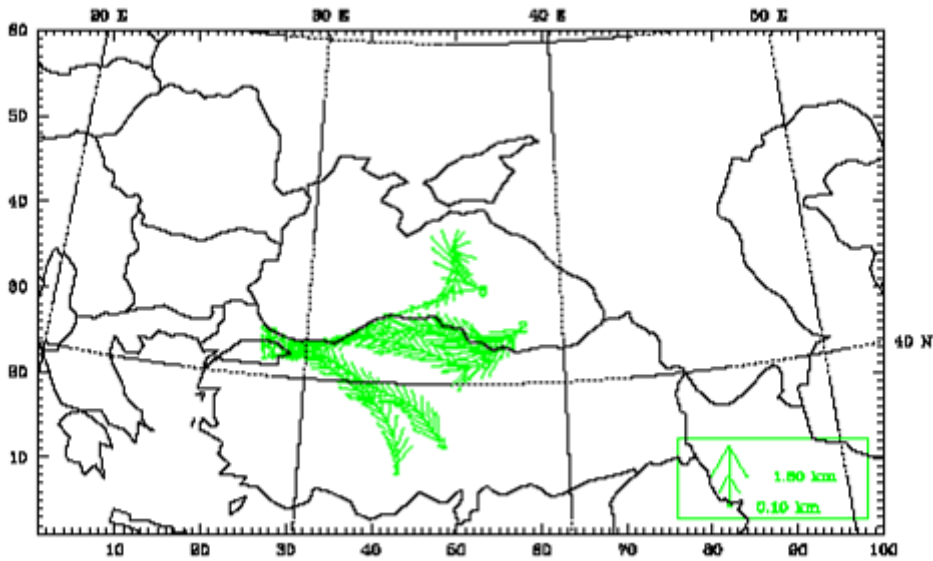


**Figure 5.9.** MM5 Forward Trajectory Approach for 23 July 2002

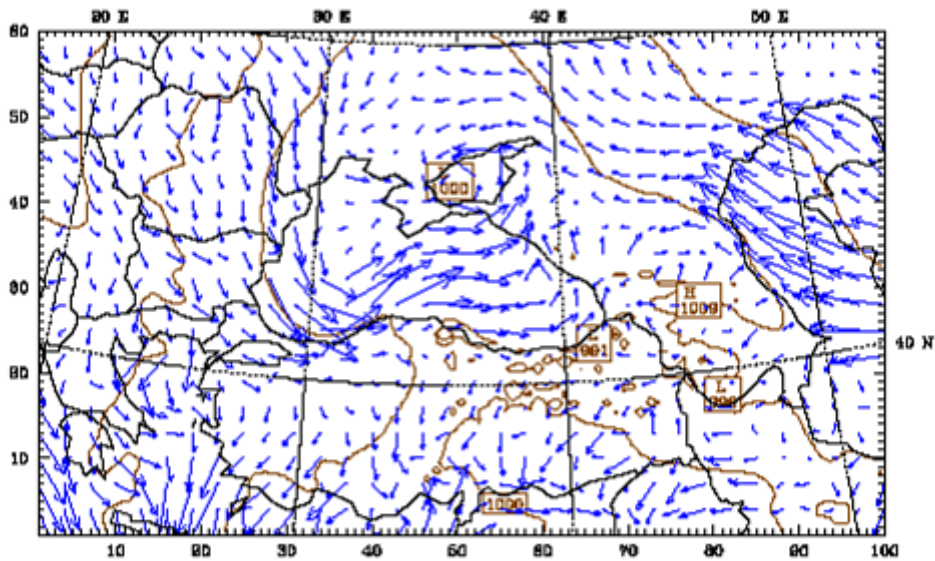


**Figure 5.10.** Wind Direction and Sea Level Pressure for 23 July 2002

Forward air trajectories generated in 23 July 2002 are presented in Figure 5.9. South-Eastern, Eastern and North-Eastern trajectories are the result of the wind directions, shown in Figure 5.10. North-Western winds come to Istanbul, from the Balkans. There is a low pressure center on Black Sea. With the impact of this center, a part of air trajectories' direction is the North-East. Besides, Eastern and South-Eastern winds may be seen on the North and mid part of Turkey. Forward trajectories can rise up to 1.80 km.

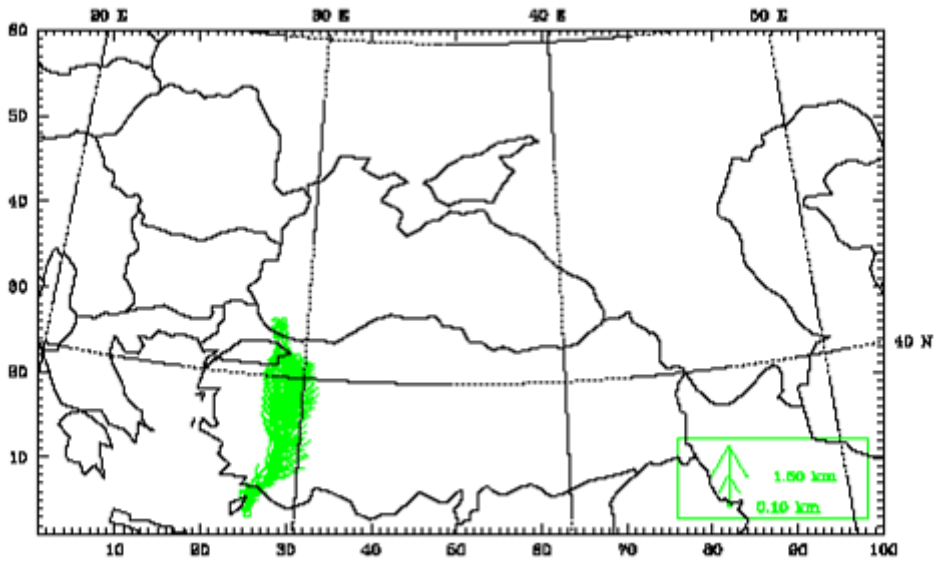


**Figure 5.11.** MM5 Forward Trajectory Approach for 24 July 2002

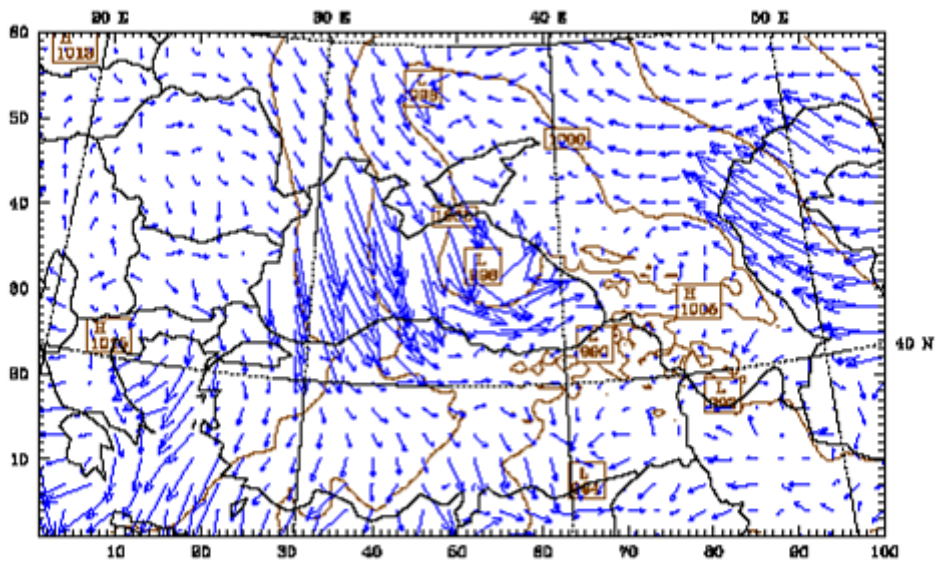


**Figure 5.12.** Wind Direction and Sea Level Pressure for 24 July 2002

Forward air trajectories generated for 24 July 2002 are presented in Figure 5.11. Trajectories are mainly towards South and South-West, as a result of the wind directions (Figure 5.12.) for the same period. Forceful Northern winds comes from the Black Sea and affects the North coastline of our country. Forward trajectories can rise up to 1.50 km. Western and North-Western winds -from the Balkans- are directed to Istanbul. In the South of Istanbul, winds blow towards the South-West.

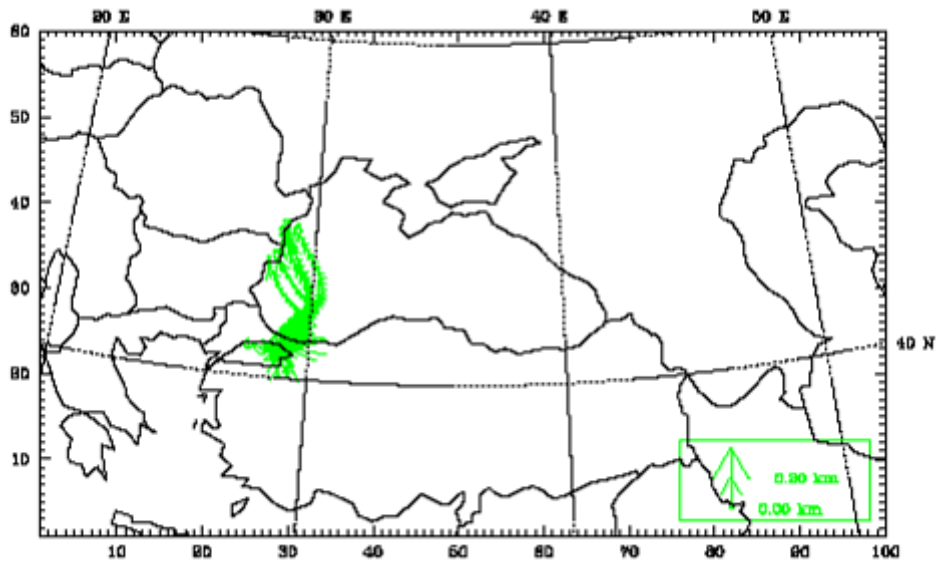


**Figure 5.13.** MM5 Forward Trajectory Approach for 25 July 2002

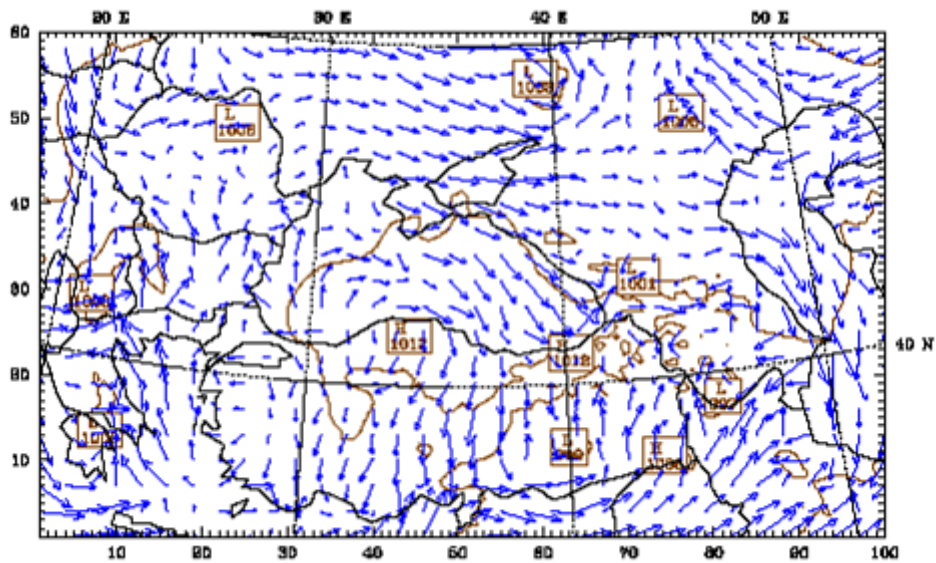


**Figure 5.14.** Wind Direction and Sea Level Pressure for 25 July 2002

Figure 5.13. shows the forward air trajectories for 25 July 2002 at 00:00. There are Eastern winds (Figure 5.14.) on Istanbul, and there is a circulation on Istanbul. Trajectories pass the Black Sea and arrive at the Black Sea coastline of Bulgaria and Romania in the end of a 24-hour period. Forward trajectories can rise up to 0.20 km.

## 6. CONCLUSIONS

Day by day, air pollution is becoming a very serious issue for all over the world and for Turkey. Especially megacities' pollution problems are rising day by day because of population growth, transportation, traffic and industrial activities. Besides their own pollution sources, long-range aerosol transport makes a contribution to the air pollution.

In this research, trans-boundary pollutant transport originating from Istanbul was assessed in terms of meteorology and trajectory approaches. Aim of this study was to show the impact of the air pollution in Istanbul to its surroundings, especially to the towns in the vicinity. A 30-year period (1961-1990) NCEP/NCAR (National Centers for Environmental Predictions/National Centers for Atmospheric Research) reanalysis data (NNRP-NCEP NCAR Reanalysis Project -2.5°, 6-hourly) was used for a comprehensive climatological trajectory evaluation. Generally, air quality models are used to estimate the air pollutant concentration (i.e CMAQ), but emission inventory for the area of interest is difficult to find and running the model is a hard and complex study that requires a long time effort. The advantage of this study is to be able to use NCEP/NCAR reanalysis data for a 30-year-period, it is impossible to run an atmospheric dispersion model for the same long period (Kindap, 2005).

The climatological trajectory studies have shown the air parcel movement from Istanbul to the selected megacities. Except summer duration, seasonal distributions are similar to the annual one. It can be said that, Istanbul's air pollution threatens to its surroundings, with the impact of main wind directions, throughout the year. Results show that the South and the South-West of Istanbul are the most affected areas from the air parcel movement of Istanbul. Izmir is the most affected city from the air pollution in Istanbul with 8496 trajectories (Probability of arrival is 20.05 %) throughout the year. And Roma is the less affected city from the air pollution in Istanbul with 238 trajectories (Probability of arrival is 0.56 %) throughout the year. Bucuresti is nearly three times closer to Istanbul than Cairo, Cairo experiences higher probability of trajectory arrival (3.43 %) than Bucuresti (1.94 %). It can be said that nine of the selected cities (Athens, İzmir,

Crete, Antalya, Sinop, Ankara, Bucuresti, Sofia and Nicosia) might be affected from the air transport of Istanbul in a two-day period.

In the second part of the study, air trajectories were generated using Fifth-Generation NCAR/Penn State Mesoscale Model (MM5) for a specific episode; 22, 23, 24, 25 July 2002 at 00:00 UTC for a 24-hour period. Wind speeds and directions are variable in these times. Trajectories generated in this episode may be different from the trajectories generated using a 30-year NCEP/NCAR reanalysis data. Air trajectories are mainly to the South in 22 July, to the East, to the South-East and North-East in 23 July, to the South and South-West in 24 July and to the North and North-West in 25 July 2002. It is obvious that, although climatological trajectory approach gives general knowledge about air transport, it is impossible to predict daily air parcel movements based on it.

Correct and detailed information about local emissions is an important requirement. The CORINAIR/EMEP emission inventory has a coarse resolution and doubtful data covering a lot of countries, including Turkey. To be able to get more accurate results, a high-resolution emission inventory is needed.

In future work, our aim is to show the concentration distributions and transportations using Air Quality Models (AQM).

## REFERENCES

- Anthes, R., A., Warner, T.T., 1978. The Development of Mesoscale Models Suitable for Air Pollution and Other Mesometeorological Studies, *Monthly Weather Review*, 106, 1045-1078.
- Becin, A., 2002. Environmental Impacts of Urban Transport, M.S. Thesis, Istanbul Technical University.
- Beychok, M.R., 2005. Fundamentals of Stack Gas Dispersion, Version 4, <http://www.air-dispersion.com>.
- Borge, R., Lumbreras, J., Vardoulakis, S., Kassomenos, P., Rodriguez, E., 2007. Analysis of Long-Range Transport Influences on Urban PM10 Using Two-Stage Atmospheric Trajectory Clusters. *Atmospheric Environment*, 41, 4434-4450.
- Brimblecombe, P., 1987. *The Big Smoke: A History of Air Pollution in London Since Medieval Times.*, U.S.A., 185.
- Builtjes, P., 2001. Major Twentieth Century Milestones in Air Pollution Modeling and Its Application. *Air Pollution Modeling and Its Application XIV*. Springer.
- Clapp, B. W., 1994 . *An Environmental History of Britain*. Longman, London.
- Dayan, U., 1986. Climatology of Back Trajectories From Israel Based On Synoptic Analysis. *Journal of Applied Meteorology*, 25, 591-595.
- Davis, R.E., Sitka, L., Hondula, D.M., Gawtry, S., Knight, D., Lee, T., Stenger, P.J., 2007. A Preliminary Back-Trajectory And Air Mass Climatology for the Shenandoah Valley, American Meteorological Society, Formerly J3.16 for Applied Climatology.
- Draxler, R.R., Hess, G.D., 1998. An Overview of the HYSPLIT\_4 Modeling System For Trajectories, Dispersion and Deposition. *Australian Meteorological Magazine*, 47, 295-308.



Ezber, Y., Sen, O.L., Kindap, T., Karaca, M., 2007. Climatic Effects of Urbanization In Istanbul: A Statistical And Modeling Analysis. *International Journal of Climatology*, 27, 667-679.

Freiwan, M., İncecik, S., 2006. Modeling European Air Pollutants Transport to the Eastern Mediterranean Region. *Bulletin of the Technical University of Istanbul*, 5, 3, 255-266.

Gertler, A.W., 2006. Development and Validation of A Predictive Model to Assess the Impact of Coastal Zone Emissions on Urban Scale Air Quality. Chairman's Air Pollution Seminar Series, Air Resources Board, California Environmental Protection Agency.

Grell, G. A., Dudhia, J., Stauffer, D. R., 1994. A Description of the Fifth Generation Penn State/NCAR Mesoscale Model (MM5). National Center for Atmospheric Research, Boulder, CO, NCAR/TN-389+STR.

Guo, Y.-R., Chen, S., 1994. Terrain and land use for the fifth-generation Penn State/NCAR mesoscale modeling system (MM5). NCAR Technical Note, NCAR/TN-397+IA, 114 pp.

[http://en.wikipedia.org/wiki/Emission\\_inventory](http://en.wikipedia.org/wiki/Emission_inventory)

Harris, J.M., 1982. The GMCC Atmospheric Trajectory Program, NOAA Technical Memorandum, ERL ARL-116, 30.

Hong, S. Y., Pan, H.L., 1996. Nonlocal Boundary Layer Vertical Diffusion In a Medium-range Forecast Model, *Mon. Wea. Rev.*, 124, 2322-2339.

Im, U., Tayanç, M., Yenigun, O., 2006. Analysis of Major Photochemical Pollutants With Meteorological Factors For High Ozone Days In Istanbul, Turkey. *Water, Air & Soil Pollution*, 175, 335-359.

Im, U., Tayanç, M., Yenigun, O., 2008. Interaction Patterns of Major Photochemical Pollutants In Istanbul, Turkey. *Atmospheric Research*, 89, 382-390.

Innocentini, V., 1999. A Successive Substitution Method for the Evaluation of Trajectories Approximating the Parcel Path by a Linear Function of Space and Time. *American Meteorological Society*, 127, 1639-1650.

Eurasia Institute of Earth Sciences (EIES), 2005. Istanbul Climate and Air Pollution Report, Istanbul Technical University.

- Jacobson, M.Z., 2002. Atmospheric Pollution: History, Science and Regulation, United Kingdom, 82-91.
- Jacobson, M.Z., Colella, W.G., Golden, D.M., 2005. Cleaning the Air And Improving Health With Hydrogen Fuel-Cell Vehicles. *Science*, 308, 1901-1905.
- Jafari, H.R., Ebrahimi, S., 2007. A Study on Risk Assessment of Benzene as one of the VOCs Air Pollution. *International Journal of Environmental Research*, 3, 214-217.
- Kanat, G., Air Pollution in Istanbul and the Importance of Heat Isolation, Yıldız Technical University, Environmental Engineering Department, <http://www.yildiz.edu.tr/~kanat/Hava.html>.
- Kindap, T., 2005. Long-Range Aerosol Transport From Europe To Istanbul, Turkey. Ph.D. Thesis, Istanbul Technical University.
- Kindap, T., Unal, A., Chen, S.-H., Hu, Y., Odman, M.T., Karaca, M., 2006. Long-range Aerosol Transport From Europe To Istanbul, Turkey. *Atmospheric Environment*, 40, 3536-3547.
- Kindap, T., 2008. Identifying the Trans-Boundary Transport of Air Pollutants to the City of Istanbul Under Specific Weather Conditions. *Water, Air & Soil Pollution*, 189, 279-289.
- Kindap, T., Turuncuoglu, U.U., Chen, S-H., Unal, A., Karaca, M., 2008. Potential Threats From A Likely Nuclear Power Plant Accident: A Climatological Trajectory Analysis And Tracer Study. *Water, Air & Soil Pollution*, 198, 393-405.
- Komuscu, A.U., 2001. An Analysis of Recent Drought Conditions In Turkey In Relation To Circulation Patterns, *Drought Network News*, 13(2-3), 5-6, 2001.
- Kostandinos, M., Im, U., Alper, U., Dimitrios, M., Yenigun, O., Incecik, S., 2009. Compilation of a High Spatially And Temporally Resolved Emission Inventory For The Istanbul Greater Area Using GIS Technology (In preparation to submit).
- Martin, D., Granier, J.P., Imbard, M., Strauss, B., 1984. Application of a Long Range Transport Model to a Mount Etna Plume. *Bulletin of Volcanology*, 47, 1097-1106.

McGowan, H. A., Kamber, B., McTainish, G.H., Marx, S.K., 2005. High Resolution Provenancing of Long Travelled Dust Deposited on the Southern Alps, New Zealand. *Geomorphology*, 69, 208-221.

Pennsylvania State University / National Center for Atmospheric Research Numerical Model Home Page,

[http://www.mmm.ucar.edu/mm5/documents/MM5\\_tut\\_Web\\_notes/tutorialTOC.htm](http://www.mmm.ucar.edu/mm5/documents/MM5_tut_Web_notes/tutorialTOC.htm)

Pettersen, S., 1956. *Weather Analysis and Forecasting*, McGraw Hill, 27-31.

Saltbones, J., Foss, A., Bartnicki, J., 2000. Threat Norway From Potential Accidents at the Kola Nuclear Power Plant; Climatological Trajectory Analysis and Episode Studies. *Atmospheric Environment*, 34, 407-418.

Sertel, E., Demirel, H., Kaya, S., Demir, I., 2008. Spatial Prediction of Transport Related Urban Air Quality. *The International Archives of the Photogrammetry, Remote Sensing and Spatial Information Sciences*. Vol. XXXVII. Part B2, Beijing.

Simpson D., Winiwarter W., Borjesson B., Cinderby S., Ferreiro A., Guenther A., Hewitt C.N., Janson R., Khalil A.M.K., Owen S., Pierce T.E., Puxbaum H., Shearer M., Skiba U., Steinbrecher R., Tarraso'n L. and Oquist M.G., 1999. Inventorying Emissions From Nature In Europe, *Journal of Geophysical Research*, 104, D7, 8113–8152.

Turkish Statistical Institute, Address Based Population Registration System, 2008, <http://www.tuik.gov.tr>.

U.S. Department of Commerce / National Oceanic and Atmospheric Administration Earth System Research Laboratory / Physical Sciences Division: <http://www.cdc.noaa.gov/cdc/data.ncep.reanalysis.html>

U. S. Environmental Protection Agency Office of Air and Radiation, 2003. A Guide to Designing And Operating a Cap And Trade Program For Pollution Control, EPA430-B-03-002, [www.epa.gov/airmarkets](http://www.epa.gov/airmarkets).

Vallero, D.A., 2008. *Fundamentals of Air Pollution*, Academic Press, 4th edition, 552-553.